

1 **Dangerous degree forecast of soil and water loss on highway slopes in**
2 **mountainous areas using the revised universal soil loss equation**

3 **Yue Li^{1,2}, Shi Qi^{*1,2}, Bin Liang^{1,2}, Junming Ma^{1,2}, Baihan Cheng^{1,2}, Cong Ma³, Yidan Qiu³,**
4 **and Qinyan Chen³**

5 ¹ Key Laboratory of State Forestry Administration on Soil and Water Conservation, Beijing
6 Forestry University, Beijing 100083, China

7 ² Beijing Engineering Research Center of Soil and Water Conservation, Beijing Forestry
8 University, Beijing 100083, China

9 ³ Yunnan Science Research Institute of Communication & Transportation, Kunming 650011,
10 China

11

12 **Abstract**

13 Many high and steep slopes are formed by special topographic and geomorphic types and
14 mining activities during the construction of mountain expressways. **Severe** soil erosion may **also**
15 occur under heavy rainfall conditions. Therefore, predicting soil and water loss on highway slopes
16 is important in protecting infrastructure and human life. In this study, we investigate Xinhe
17 Expressway located **at** the southern edge of the Yunnan–Guizhou Plateau. The revised universal
18 soil loss equation is **used** as the prediction model for soil and water loss on slopes. **Geographic**
19 information systems, remote sensing technology, field surveys, runoff plot observation testing,
20 cluster analysis and co-kriging calculations are **also utilised**. The partition of the prediction units
21 of soil and water loss on the expressway slope in the **mountainous** area and the spatial distribution
22 of **rainfall on a** linear highway are studied. **Given** the particularity of the expressway slope in the
23 **mountainous** area, **the model parameter** is modified, and the risk of soil and water loss along the
24 mountain expressway is simulated and predicted under 20- and 1-year rainfall return periods. The
25 **following** results are **obtained**. (1) Natural watersheds can be considered for the prediction of
26 slope soil erosion to represent the actual situation of soil and water loss **on** each slope. Then, the
27 spatial location of **the** soil erosion unit can be **determined**. (2) **Analysis** of actual observation data
28 shows that the overall average absolute error of the monitoring area is $33.24 \text{ t}\cdot\text{km}^{-2}\cdot\text{a}^{-1}$, the overall
29 average relative error is 33.96% and the overall root mean square error is between 20.95 and 65.64,
30 all of which are within acceptable limits. The Nash efficiency coefficient is 0.67, **indicating** that
31 the prediction accuracy of the model satisfies the requirements. (3) Under the 1-year rainfall
32 **condition**, we find **through** risk classification that the percentage of prediction units with no risk of
33 erosion is 78%. **The soil** erosion risk is low and does not affect road traffic safety. Under the 20-
34 year rainfall condition, the percentage of units with high and extremely high **risks** is 7.11%. The
35 prediction results can help adjust the **design** of water and soil conservation measures for these

36 units.

37 **Keywords:** Soil and water loss; highway slopes; mountainous areas; RUSLE;
38 dangerous degree forecast

39

40 **Introduction**

41 China has gradually accelerated its construction of highways in recent years, improved its
42 transportation networks and promoted rapid economic development (Jia et al., 2005). With the
43 implementation of the Western development strategy, advanced requirements for the construction
44 of expressways have been proposed to connect coastal plains and inland mountains. However,
45 many unstable high and steep slopes, such as natural, excavation and fill slopes, are inevitably
46 formed by the frequent filling and deep digging along expressways in mountain areas.

47 The slope is the most fragile part of an expressway in a mountain area. During rainy seasons,
48 soil erosion is easily caused by rainwash and leads to considerable damage (Figure 1). At present,
49 China's highway industry remains in a period of rapid development. At the end of 2014, the total
50 mileage of highway networks exceeded 4,400,000 km, whilst that of expressways was 112,000 km
51 (Yuan et al., 2017; Mori et al., 2017; Kateb et al., 2013; Zhou et al., 2016). Statistics further
52 indicate that in the next 20–30 years, the expressways in China will have a total length of more
53 than 40,000 km. For every kilometre of highway, the corresponding bare slope area is expected to
54 reach 50,000–70,000 m² (Wang, 2006). The annual amount of soil erosion is 9,000 g/m³, which
55 can cause 450 t of soil loss annually (Chen, 2010). The soil and water loss of roadbed slopes
56 differs from the soil and water loss in woodlands and farmlands. Forestlands and farmlands are
57 generally formed after years of evolution and belong to the native landscape. Most of the slopes of
58 these land types are gentle and stable (Kateb et al., 2013). Moreover, traditional soil and water
59 conservation research has focused on slopes with 20% grade or below, but roadbed slopes of
60 highways generally have a grade of 30% or above (Zhou, 2010). Soil erosion on roadbed side
61 slopes affects not only soil and water loss along highways but also road operation safety (Gong
62 and Yang, 2016; Jiang et al., 2017). Therefore, soil erosion on the side slopes of mountain
63 expressways must be studied to control soil erosion, improve the ecological environment of
64 expressways and realise sustainable land utilisation (Wang et al., 2005; Yang and Wang, 2006).

65 The revised universal soil loss equation (RUSLE) is a set of mathematical equations used to
66 estimate the average annual soil loss and sediment yield resulting from inter-rill and rill erosion
67 (Renard et al., 1997; Foster et al., 1999; Zerihun et al., 2018; Toy et al., 2002). RUSLE was
68 derived from the theory of erosion processes and has been applied to more than 10,000 plot-years
69 of data from natural rainfall plots and numerous rainfall-simulation plots. RUSLE is an
70 exceptionally well-validated and documented equation. It was conceptualised by a group of
71 nationally recognised scientists and soil conservationists with extensive experience in erosion

72 processes (Soil and Water Conservation Society, 1993).

73 The use of RUSLE models as predictive tools for the quantitative estimation of soil erosion
74 has matured (Panagos et al., 2018; Cunha et al., 2017; Taye et al., 2017; Renard, 1997). The range
75 of application of these models involves nearly every aspect of soil erosion. Moreover, many
76 scientists have conducted useful explorations to modify the model's parametric values and
77 improve its simulation accuracy.

78 Tresch et al. (1995), in a study in Switzerland, argued that slope length (L) and slope
79 steepness (S) are crucial factors in soil erosion prediction, and these parameters significantly
80 influence the erosion values calculated by RUSLE. All existing S factors can be derived only from
81 gentle slope inclinations of up to 32%; however, many cultivated areas are steeper than this
82 critical value. A previous study used 18 plot measurements on transects along slopes with
83 steepness from 20% to 90% to qualitatively assess the most suitable S factors for steep subalpine
84 slopes; the results showed that the first selection of the S factor is possible for slopes beyond the
85 critical steepness of 25% (Tresch et al., 1995). Rick et al. (2001) found that using universal soil
86 loss equation (USLE) and RUSLE soil erosion models at regional landscape scales is limited by
87 the difficulty of obtaining an LS factor grid suitable for geographic information system (GIS)
88 applications. Therefore, their modifications were applied to the previous arc macro language
89 (AML) code to produce a RUSLE-based version of the LS factor grid. These alterations included
90 replacing the USLE algorithms with their RUSLE counterparts and redefining the assumptions on
91 slope characteristics. In areas of western USA where the models were tested, the RUSLE-based
92 AML program produced LS values that were roughly comparable to those listed in the RUSLE
93 handbook guidelines (Rick et al., 2001). Silburn (2011) showed that estimating the soil erodibility
94 factor (K) from soil properties (derived from cultivated soils) provides a reasonable estimate of K
95 for the main duplex soils at the study site as long as the correction for undisturbed soil is used to
96 derive K from the measured data before application to the USLE model (Silburn, 2011). Wu (2014)
97 adopted GIS and RUSLE methods to analyse the risk pattern of soil erosion in the affected road
98 zone of Hangjinq Highway in Zhuji City, Zhejiang Province. Digital elevation model (DEM)
99 data, rainfall records, soil type data, remote sensing imaging and a road map of Hangjinq
100 Highway were used for GIS and RUSLE analyses (Wu et al., 2014). Chen (2010), who initially
101 considered the terrain characteristics of roadbed side slopes and conducted a concrete analysis of
102 the terrain factor calculation method in RUSLE, evaluated a compatible terrain factor
103 computational method of roadbed side slopes and proposed a revised method based on the
104 measured data of soil erosion in the subgrade side slope of Hurongxi Expressway (from Enshi to
105 Lichuan) in Hubei Province. The results indicated that (1) the slope length factor in RUSLE can
106 be calculated by $L = \left(\frac{\lambda}{22.1}\right)^m$, but m should not be computed by using the original method for
107 highway subgrade side slope because its gradient surpasses the generally applicable scope of
108 RUSLE. Moreover, (2) the slope length factor (L) of the highway subgrade side slope can be

109 calculated by $L = \left(\lambda/22.1\right)^{0.35}$ (Chen et al., 2010). Zhang (2016) investigated the spatiotemporal
110 distribution of soil erosion in a ring expressway before and after construction by using a land
111 use/cover map of Ningbo City in 2010. The topographic map of the North Ring Expressway and
112 field survey data were collected for the DEM. Rainfall data were also collected from local
113 hydrological stations. On the basis of the collected data, the spatial distribution of the factors in
114 the RUSLE model was calculated, and soil erosion maps of the North Ring Expressway were
115 estimated. Then, the soil erosion amount was calculated at three different stages by RUSLE. The
116 results showed that slight erosion was dominant during the preconstruction and natural recovery
117 periods, which accounted for 98.53% and 99.73%, respectively. During the construction period,
118 mild erosion and slight erosion had the largest values and accounted for 52.5% and 35.4%,
119 respectively. Soil erosion during the construction period was mainly distributed in temporary
120 ground **soil** (Zhang et al., 2016).

121 However, the common methods used to fit the parameters can affect the findings, and
122 minimising the sum of the squares of errors for soil loss may provide better results than simply
123 fitting an exponential equation. Yang (2014) found that the *C* factor, as a function of fractional
124 bare soil and ground cover, can be derived from MODIS data at regional or catchment scales. The
125 method offered a meaningful estimate of the *C* factor for determining ground cover impact on soil
126 loss and erosion hazard areas. The method **performed** better than commonly used techniques based
127 on green vegetation **only** (e.g. normalised difference vegetation index (NDVI)), and it was
128 appropriate for estimating the vegetation cover management factor (*C*) in the modelled hillslope
129 erosion in New South Wales, Australia by using emerging fractional vegetation cover products.
130 Moreover, the approach effectively mapped the spatiotemporal distribution of the RUSLE cover
131 factor and the hillslope erosion hazard in a large area. The methods and results described in this
132 previous work are **important in** understanding the **spatiotemporal** dynamics of hillslope erosion
133 and ground cover. According to Kinnell (2014), runoff production, which is spatially uniform, is
134 often inappropriate under natural conditions because infiltration is spatially variable. **Upslope**
135 length varies with the ratio of the upslope runoff coefficient to the runoff coefficient for the area
136 below the downslope boundary of the segment in the modified RUSLE approach. **The use of**
137 **upslope length** produces only minor variations in soil loss compared with **using values** predicted
138 by the standard RUSLE approach when the runoff is spatially variable and the number of
139 segments increases. By contrast, the USLE-M approach can predict soil loss that is influenced
140 strongly by runoff when runoff varies in space and time. Therefore, an increase in runoff through a
141 segment causes an increase in soil loss, **and** a decrease in runoff through a segment or cell results
142 in a decrease in soil loss.

143 In general, past studies (e.g. Tresch et al., 1995; Rick et al., 2001; Silburn, 2011; Yang, 2014;
144 Kinnell, 2014) focused on sloping fields, but the research on soil erosion on highway slopes is
145 limited. Subgrade slope is a major part of soil erosion during construction and operation periods.

146 Therefore, soil erosion caused by subgrade slope should be predicted. However, the research on
147 soil and water loss of highways hardly meets the requirements of practical work (Xu et al., 2009;
148 Bakr et al., 2012). We still need to conduct considerable work on the prediction of soil erosion on
149 highway slopes. The situation in various regions in China indicates that researchers have helped
150 improve the RUSLE model and studied soil erosion in certain areas. Water and soil erosion caused
151 by engineering construction is an important aspect of research, especially from the perspective of
152 agricultural cultivation and forestry deforestation, because the amount of eroded soil produced by
153 embankment slopes accounts for a large proportion of the entire project area. Although this
154 concern is related to project feasibility and cost in particular, the topic has elicited considerable
155 interest in general. Furthermore, the principal factor that causes soil erosion on slopes generally
156 corresponds to precipitation amount and embankment width. Wang (2005) established several
157 experimental standardised spots for soil loss collection on the side slopes of the Xiaogan–Xiang
158 Fan Freeway (i.e. under construction thus far) and installed an on-the-spot rainfall auto-recorder.
159 The collected data were used for the revision of the main parameters R (rainfall and runoff) and K
160 (erodibility of soil) of USLE, which is widely applied to forecast soil loss quantity in plowlands
161 and predict the soil loss quantities of different types of soil on side slopes disturbed by engineering
162 treatments (Wang et al., 2005). This method not only applies to the prediction of disturbed soil
163 loss during expressway construction but also improves prediction accuracy. It also provides
164 scientific support for relevant units or personnel to implement reasonable preventive measures.

165 Related literature indicates that research on soil and water loss in highways has the following
166 limitations. First, most of the studies on C and P factors that used the RUSLE model were
167 conducted by referring to previous research results, and data accuracy is often poor. Second, most
168 studies on rainfall erosivity (R) factors are limited to sloping fields, and the rainfall erosivity
169 factors of expressway slopes in mountain areas have rarely been studied. Third, slope soils in
170 highways differ depending on soil arability, and the slopes also vary. Thus, accurately predicting
171 the soil loss of different types of subgrade slopes by using the traditional K factor calculation
172 method is difficult.

173 Previous studies have shown that the spatial interpolation method of precipitation is
174 unsuitable for the study of the spatiotemporal distribution of precipitation in mountain areas (Liu
175 and Zhang, 2006). The problem involves two aspects. From the timescale perspective, the
176 characteristics of rainfall distribution and the influencing factors are not fully considered. From
177 the spatial scale perspective, the spatial heterogeneity of the region is ignored. Furthermore, many
178 studies have limited the factors that affect precipitation to altitude factors, leading to low
179 interpolation accuracy (Zhao et al., 2011; Liu et al., 2010). Thus, in this study, we consider the
180 spatial heterogeneity of linear engineering of the expressway. The rainfall factor is spatially
181 interpolated to compensate for the following limitations: shortage of rainfall data on mountain
182 areas, difficulty of representing the rainfall data of an entire expressway by using data from a
183 single meteorological station, and uneven spatial distribution and strong heterogeneity of rainfall

184 in mountain areas (Li et al., 2017). We analyse the characteristics of soil erosion to improve
185 certain aspects of expressway construction on the basis of previous research. We divide a highway
186 slope into natural and artificial units and calculate the amount of soil loss from the slope surface to
187 the pavement based on the slope surface catchment unit. The findings can be popularised because
188 this approach is in line with the actual situation. Next, we modify the parameters of the artificial
189 slope through an actual survey, runoff plot observation and other methods, and the parameters of
190 the artificial slope are corrected by referring to the form of the project and the utilised materials.
191 We not only scientifically predict the amount of soil erosion caused by highway construction in
192 mountain areas but also provide a scientific basis for the prevention and control of soil erosion and
193 rational allocation of prevention and control measures. The safe operation of highways and the
194 virtuous cycle of the ecological environment should be ensured to promote the sustainable
195 development of the local economy.

196 1 Study area

197 Xinhe Expressway is in the southern margin of the Yunnan–Guizhou Plateau, which is in
198 southeast Yunnan Province, Honghe Prefecture and Hekou County. This highway was the first in
199 Yunnan to cross the border. Thus, it has become an important communication channel between
200 China and Vietnam and possesses an important strategic and economic value. The highway is at
201 longitude 103° 33' 45"–103° 58' 32" and latitude 22° 31' 19"–22° 51' 48" (Figure 2, 3, 4) The
202 expressway stretches roughly from northwest to southeast, and its total length is 56.30 km. The
203 climate type belongs to subtropical mountain, seasonal monsoon forest and humid heat climate
204 categories. Between May and the middle of October, the area experiences wet season
205 characterised by abundant rainfall, concentrated precipitation and increased rain at night time; the
206 variation of precipitation is 400–2000 mm, whilst most regions have 800–1800 mm (Fei et al.,
207 2017; Zhang et al., 2017). During the rest of the year, the area undergoes dry season. The starting
208 point of Xinhe Expressway is in Hekou County, New Street (pile number K83+500), at an altitude
209 of 296 m. The endpoint is in the estuary of Areca Village (pile number K139+800) at an altitude of
210 95 m. The mountains along both sides are 200–380 m above sea level. The topography of the hilly
211 area in the northern part of Xinhe Expressway is complicated. The slopes on both sides rise and
212 fall, and most of the valleys constitute V- and U-shaped sections. The natural slopes on both sides
213 are mostly below 30°. The southern part of the highway has a relatively flat terrain and a gentle
214 slope. The slopes of most hills on both sides are less than 15°, and the overall height difference is
215 less than 100 m. The vegetation in the southern part of Xinhe Expressway includes tropical
216 rainforests and tropical monsoon forests, whilst that in the northern part of China is classified as
217 south subtropical monsoon evergreen broad-leaved forest. In recent years, the original vegetation
218 in this area has been reclaimed as farmland and is now planted with rubber, banana, pineapple and
219 pomegranate, which are sporadic tropical rainforest survivors. The project area along Xinhe
220 Expressway is an economic forest belt with a single vegetation type and mainly has rubber, forest

221 and other economic trees. The soil types along the highway are rich and mainly **comprise** red,
222 leached cinnamon, grey forest and grey cinnamon soils.

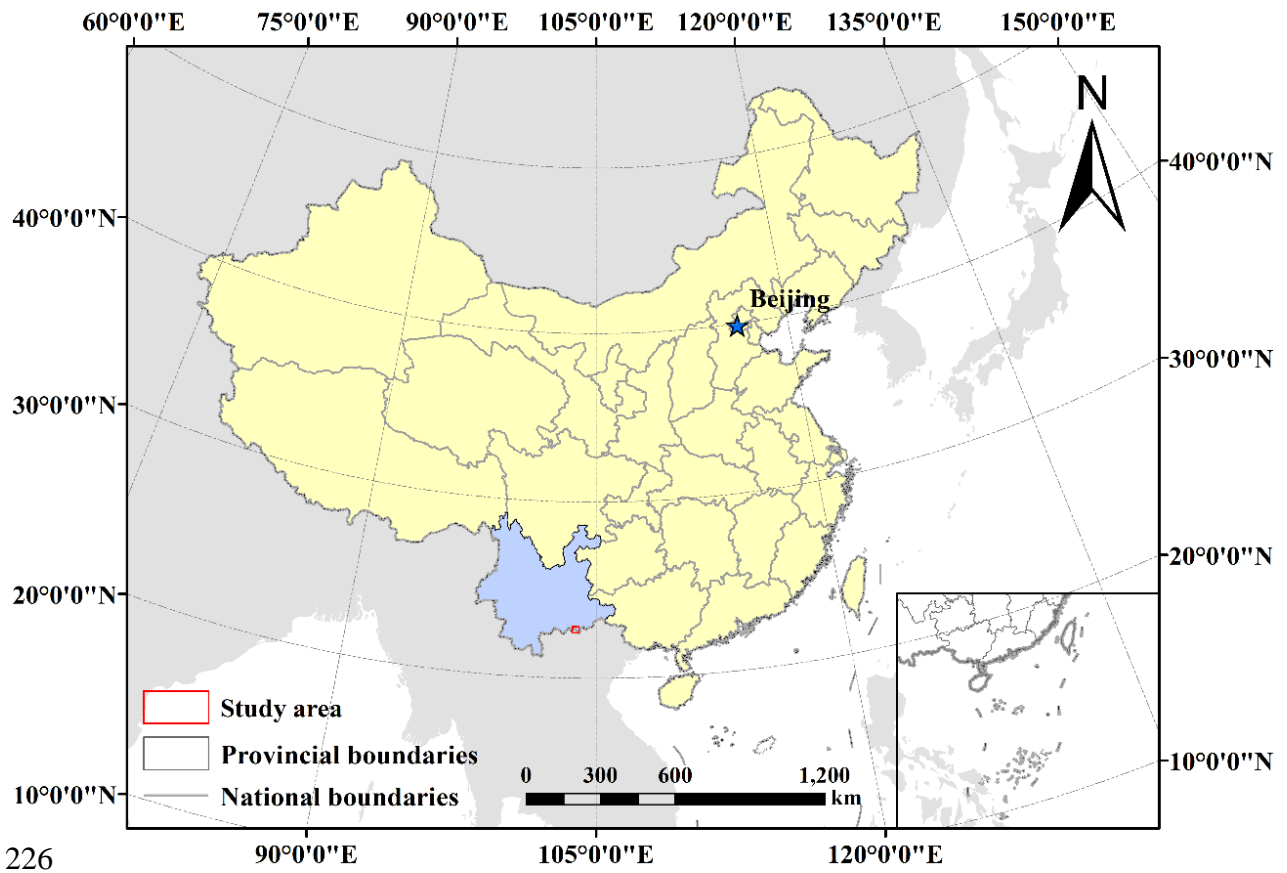


223

224

Figure 1. Soil erosion produced by rainwash on a slope after rainfall

225



226

227

Figure.2 The location of study areas in China

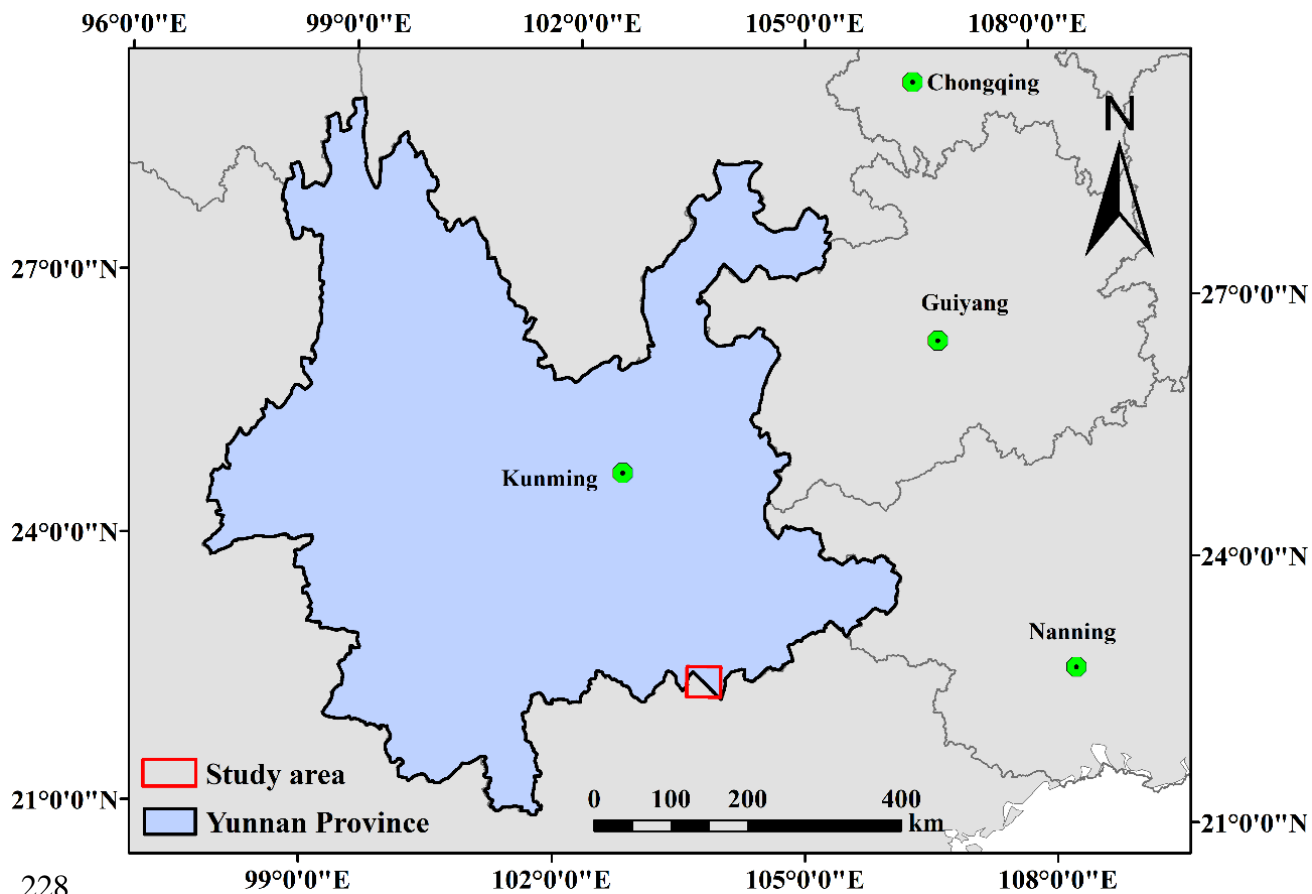


Figure.3 The location of the study areas in Yunnan Province

228

229

230

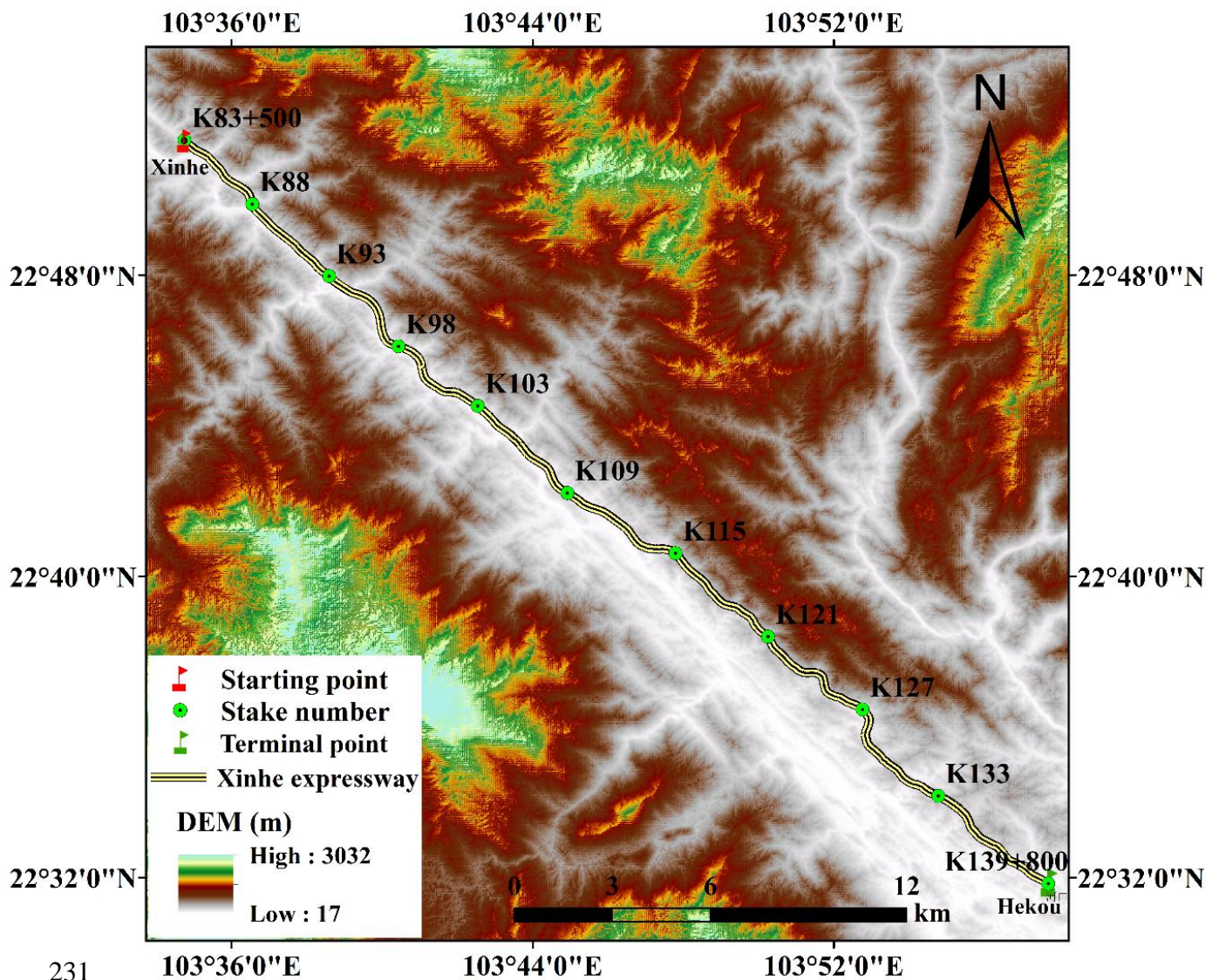


Figure.4 Overview of the study region

231

232

233

234 2 Materials and methods

235 2.1 Data sources

236 Rainfall data from 2014 were obtained from Hekou Yao Autonomous County, Pingbian Miao
 237 Autonomous County, Jinping Miao Yao Autonomous County and the meteorological department
 238 of Mengzi. The rainfall data were obtained at 5 min intervals. Meanwhile, two automatic weather
 239 stations were established along Xinhe Expressway to gather weather data during the 2014
 240 experiment. Meteorological data, which were provided by the China Meteorological Data
 241 Network, covered the period of 1959–2015 (<http://data.cma.cn/site/index.html>).

242 Data on soil types were provided by Yunnan Traffic Planning and Design Institute. Data on
 243 soil texture and organic matter were obtained via field surveys, data sampling and processing

244 methods. Soil samples were initially collected at each 1 km range of the artificial and natural
245 slopes on both sides of the highway. Five mixed soil samples were obtained from one slope by
246 using the 'S'-shaped sampling method (Shu et al., 2017). Then, the method of coning and
247 quartering was adopted (Oyekunle et al., 2011), and half of the mixed soil samples were brought
248 to the laboratory for analysis. Finally, 186 soil samples were obtained. After the soil samples were
249 dried and sieved, soil texture and organic carbon content were measured via specific gravity speed
250 measurement and potassium dichromate external heating, respectively.

251 The topographic map and design drawings of Xinhe Expressway were provided by the
252 Traffic Planning and Design Institute of Yunnan Province. The 1:2000 scale of the topographic
253 map coordinate system was based on the 2000 GeKaiMeng urban coordinate system, the elevation
254 system for 1985 national height data and the format for the CAD map in DWG. The remote
255 sensing images used in this study were derived from 8 m hyperspectral images produced by the
256 GF-1 satellite (<http://www.rscloudmart.com/>).

257

258 2.2 Prediction model selection

259 The RUSLE equation (Renard et al., 1997) was used to predict soil and water loss on the side
260 slopes of Xinhe Expressway. The RUSLE equation considers natural and anthropogenic factors
261 that cause soil erosion to produce comprehensive results. The parameters are easy to calculate, and
262 the calculation method is relatively mature. The RUSLE model is suitable for soil erosion
263 prediction in areas where physical models are not required. Formula (1) is expressed as

$$264 \quad A = R \cdot K \cdot L \cdot S \cdot C \cdot P, \quad (1)$$

265 where A is the average soil loss per unit area by erosion (t/hm^2), R is the rainfall erosivity factor
266 ($MJ \cdot mm / (hm^2 \cdot h)$), K is the soil erodibility factor ($t \cdot hm^2 \cdot h / (hm^2 \cdot MJ \cdot mm)$), L is the slope length
267 factor, S is the steepness factor, C is the cover and management practice factor and P is the
268 conservation support practice factor. The values of L , S , C and P are dimensionless.

269

270 2.3 Division and implementation of the prediction unit

271 Geological structures and rock and soil categories are complex because of considerable
272 changes in topography and physiognomy. The forms of slopes also vary. In general, according to
273 the relationship between slope and engineering, slopes can be natural or artificial. Artificial slope
274 formations can be subdivided into slope embankments and cutting slopes. In this study, we used
275 ArcGIS software to convert the topographic map of the highway design into a vectorisation file
276 because the artificial and natural slopes of watershed catchments are the main components of soil
277 erosion prediction. On the basis of the extracted graphical units, the natural and artificial slopes

278 were divided into uniform prediction units according to aspect, slope, land use and water
279 conservation measures. The aspect, slope, land use, water conservation measures and other
280 attributes of each prediction unit were consistent.

281

282 3 Results and analysis

283 3.1 Natural slope catchment area

284 The catchment unit of the slope was initially constructed by using the structural plane tools of
285 ArcGIS combined with ridge and valley lines and artificial slope and highway boundaries
286 (Zerihun et al., 2018). After the completion of the catchment unit, the slope was divided according
287 to soil type data (Table 1). After the division and overlaying of the remote sensing image map, the
288 land use types and soil and water conservation measures were considered as indicators for the
289 visual interpretation of the field survey results and for further classification of the confluence units.
290 The partition units were amended by using the vegetation coverage data obtained along Xinhe
291 Expressway. A total of 814 natural slope catchment prediction units were divided.

292

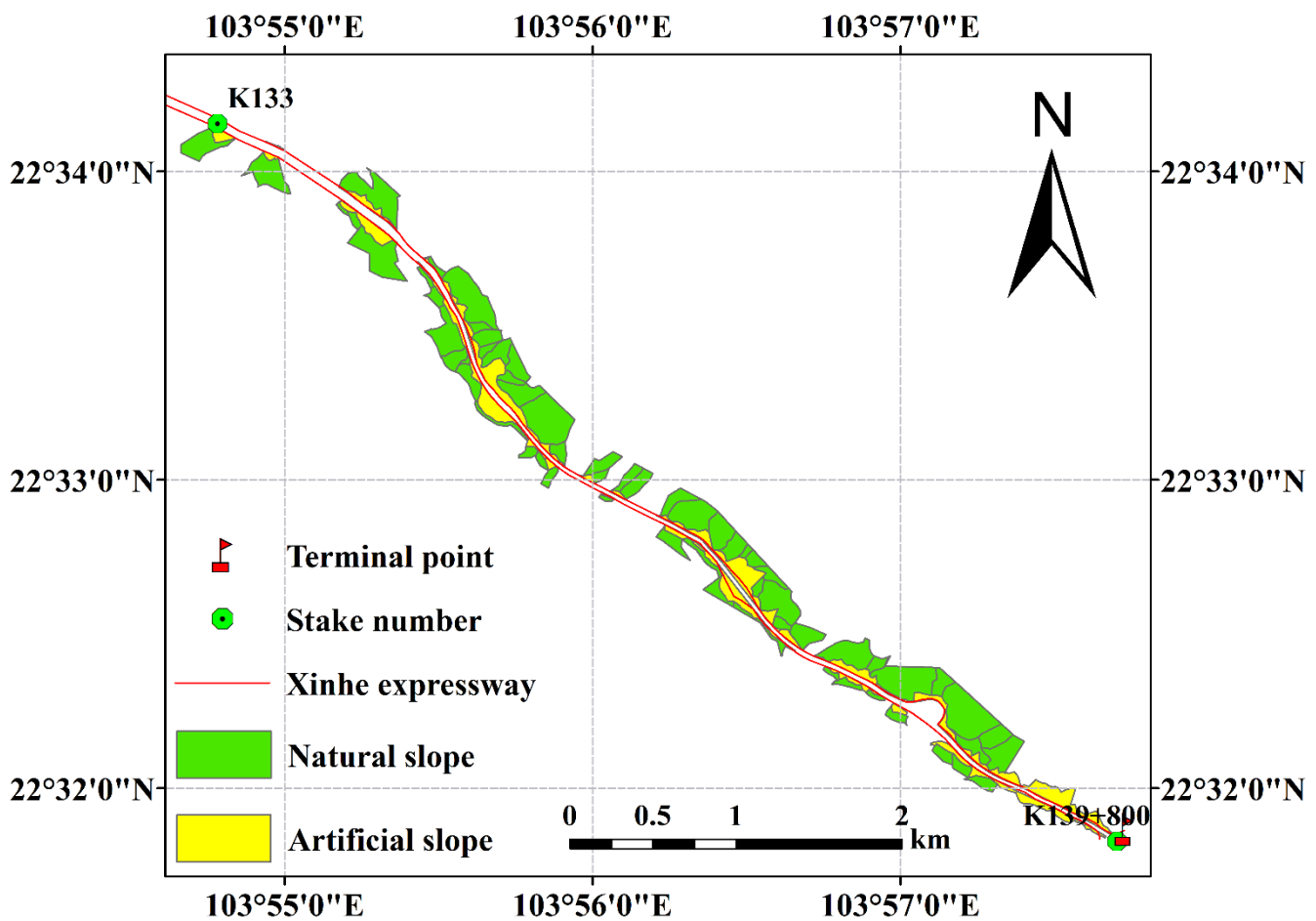
Table 1. Distribution of soil types along Xinhe Expressway

Section of the expressway	Soil type
K83+500~K84+900	latosolic red soil
K85+200~K93+200	leached cinnamon soil
K93+200~K95+900	grey forest soil
K96+900~K97+800	grey cinnamon soil
K97+800~K100+500	leached cinnamon soil
K100+500~K101+100	grey cinnamon soil
K101+100~K104	leached cinnamon soil
K104~K109+100	grey cinnamon soil
K109+100~K139	leached cinnamon soil

293

294 The artificial slope was divided into roadbed and cutting slopes according to the design of
295 Xinhe Expressway (i.e. 1:1.5 and 1:1.0 slopes). After the preliminary division, the slope
296 measurements, data design and field survey results were used as a basis for the subsequent

297 detailed division of the artificial slope into cement frame protection and six arris brick revetments.
 298 McCool (1987) stated that slope length can vary within a 10 m range and **only** has a small effect
 299 on results. The specifications of each frame in the cement frame protection along Xinh
 300 Expressway were the same. The horizontal projection length of a cement frame can be regarded
 301 the slope length value of an artificial slope. Therefore, the slope length of the artificial slope of
 302 each frame of the cement revetment was considered the same, and the value was set to 0.
 303 According to investigations, the vegetation coverage of artificial slopes with different plant
 304 species varies **substantially**. To achieve an accurate prediction of unit division and improve
 305 prediction accuracy, the artificial slopes should be continuously classified according to plant
 306 species. Thus, 422 artificial slope prediction units were obtained. The data of the 1236 slope
 307 prediction units were edited by using GIS. The results are shown in **Figure 5**.



308 **Figure 5.** Division results of the prediction units (A subset-6.8 km)

309

310 3.2 Determination of conventional parameters of the RUSLE model

311 3.2.1 Rainfall erosivity factor (*R*) (Panagos et al., 2017)

312 The formula of the *R*-value (rainfall erosivity) was adopted (Wang et al., 1995; Liu et al.,

1999; Yang et al., 1999) and calculated by using 30 min rainfall intensity as the measure, as shown in Formulas (2) and (3).

$$R = 1.70 \cdot (P \cdot I_{30} / 100) - 0.136 \quad (I_{30} < 10 \text{ mm/h}), \quad (2)$$

$$R = 2.35 \cdot (P \cdot I_{30} / 100) - 0.523 \quad (I_{30} \geq 10 \text{ mm/h}), \quad (3)$$

where R is rainfall erosivity ($\text{MJ} \cdot \text{mm} / (\text{hm}^2 \cdot \text{h})$), P is sub-rainfall (mm) and I_{30} is the maximum 30 min rainfall intensity ($\text{mm} \cdot \text{h}^{-1}$).

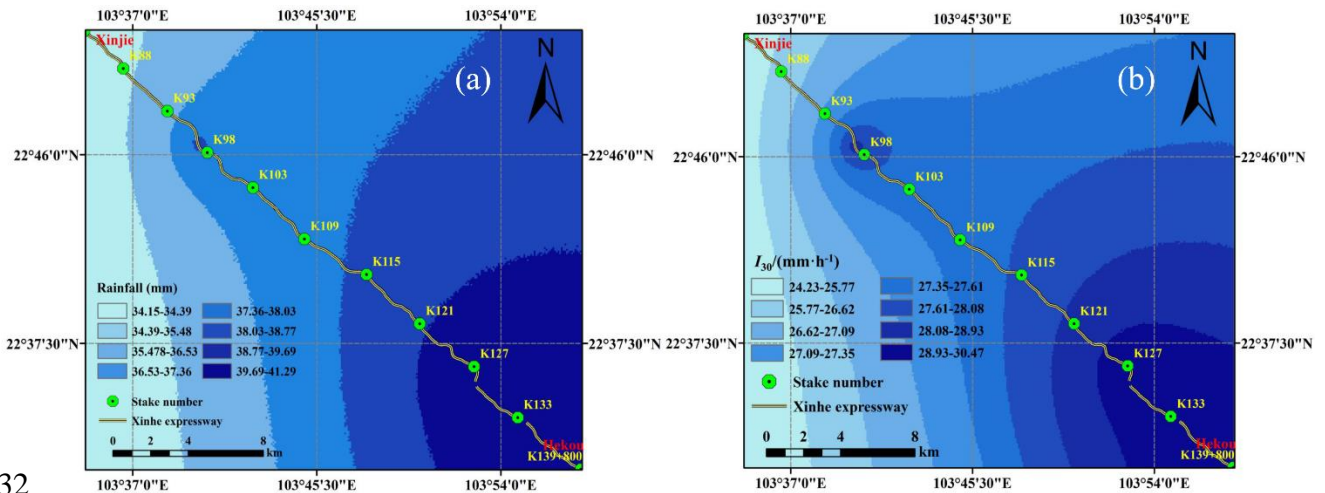
Rainfall data were acquired from stationary ground meteorological stations. However, using data from a single meteorological station to represent the rainfall data of a linear mountain expressway is difficult. The P and I_{30} values along the highway were obtained by co-kriging calculations. The dataset included the following: rainfall data; 30 min rainfall data from the four meteorological stations in Hekou Yao Autonomous County, Pingbian Miao Autonomous County, Jinping Miao Yao Autonomous County and Mengzi City; and data acquired from two automatic weather stations along the highway. Then, the cross-validation method was used to evaluate the accuracy of the interpolation results. The selection criteria included the standard root mean square error and the mean standard error. The detailed results are shown in Table 2. However, this work shows only the interpolated results of secondary rainfall of two rainfall events and the 30 min rainfall intensity data, as shown in Figures 6(a) and 6(b).

Table 2. Interpolation error of P and I_{30} values

Time of the second rainfall	P		I_{30}	
	RMSS	MS	RMSS	MS
2014.06.05	1.02	-0.02	1.06	-0.05
2014.06.07	1.04	-0.02	1.01	0.02
2014.06.17	1.09	0.03	1.11	0.06
2014.06.28	1.11	0.07	1.05	-0.03
2014.07.01	1.10	0.04	1.06	-0.04
2014.07.13	1.03	-0.02	1.01	0.02
2014.07.20	1.01	0.01	1.05	0.02
2014.08.02	1.03	0.03	0.94	0.02

2014.08.12	1.05	-0.03	1.10	0.03
2014.08.26	1.03	0.01	0.97	0.03
2014.08.29	1.09	-0.02	1.03	-0.02
2014.09.02	1.07	0.03	1.05	0.02
2014.09.04	0.96	-0.02	0.97	-0.02
2014.09.17	1.07	-0.03	1.09	-0.03
2014.09.20	0.98	0.05	1.03	0.02
2014.10.05	1.02	0.03	1.04	0.03

331



332

333

Figure 6(a). Interpolation results of secondary rainfall for June 5, 2014

334

Figure 6(b). Interpolation results of I_{30} for June 5, 2014

335

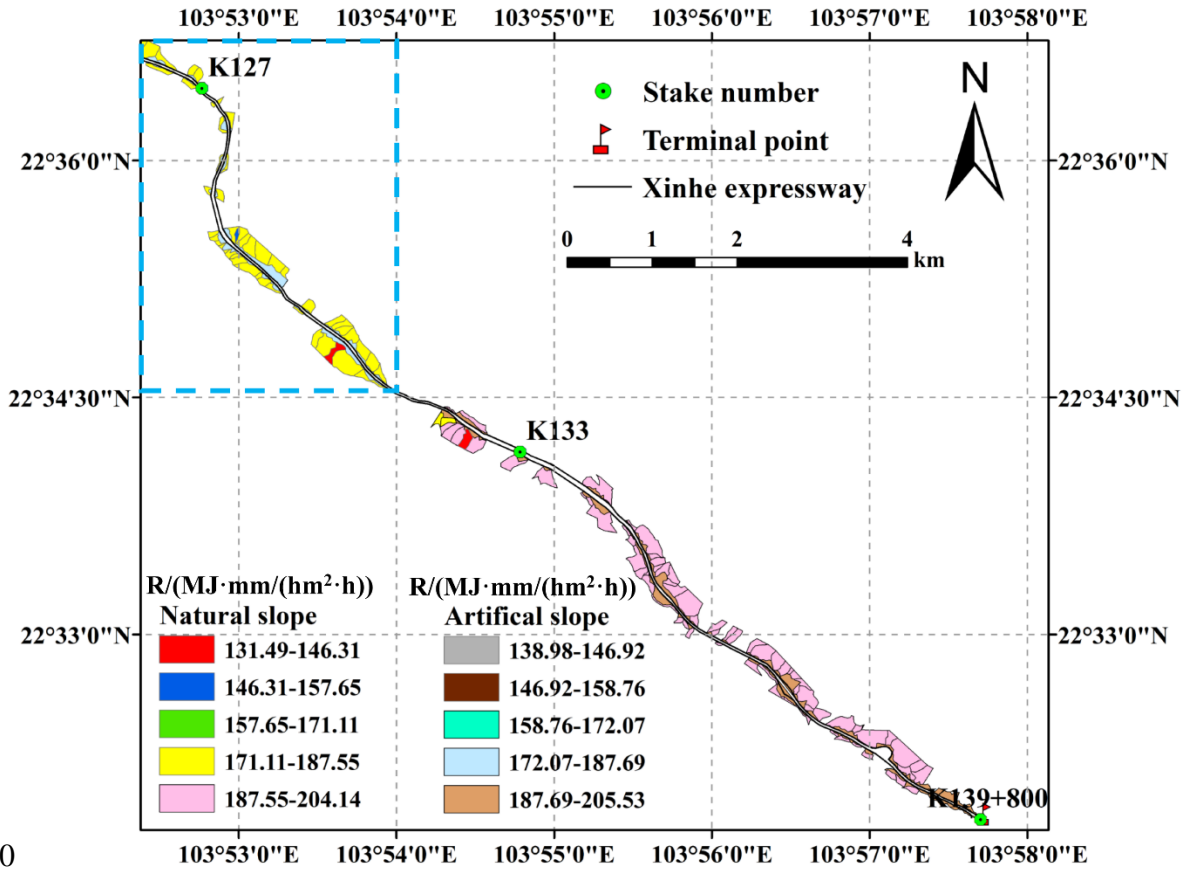
336

337

338

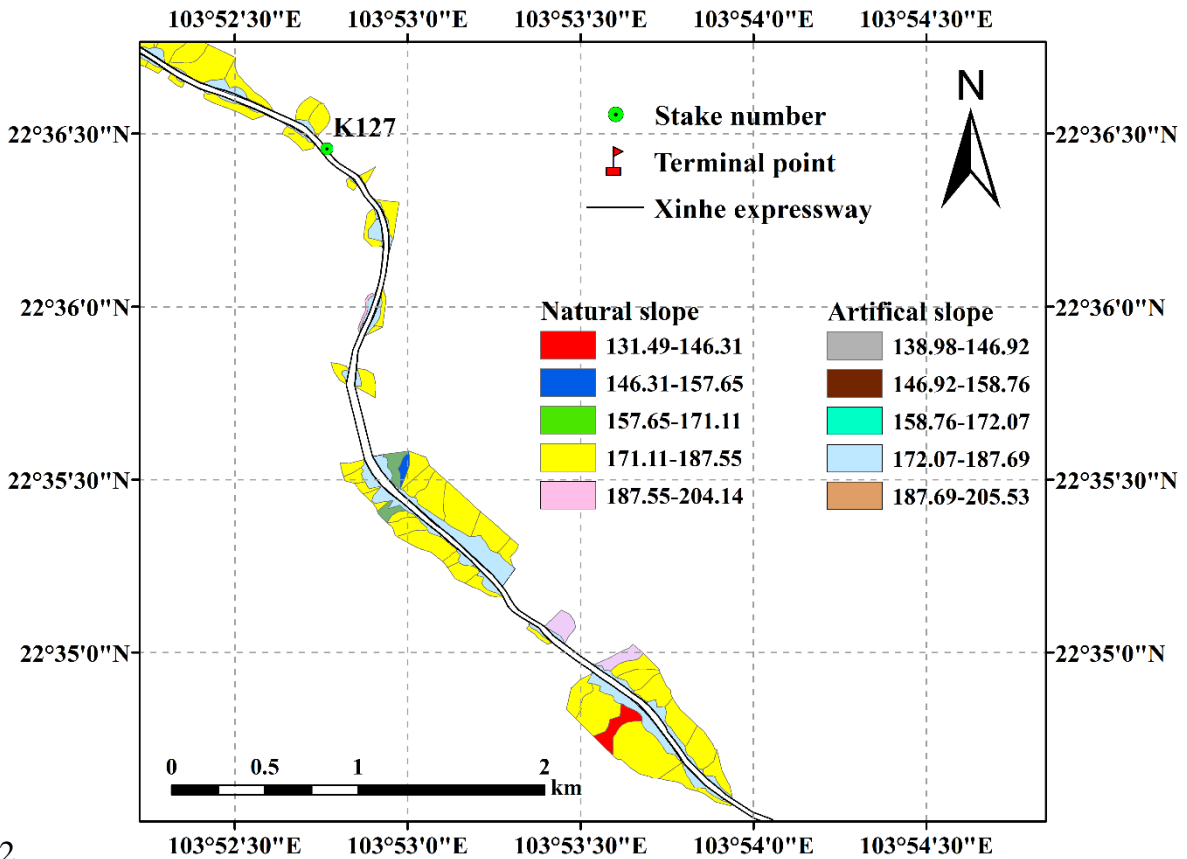
339

The secondary rainfall data of 16 rainfall instances along Xinhe Expressway were obtained by interpolation because the values for internal rainfall and the rainfall intensity of a single prediction unit are the same. Therefore, the R -value was calculated by using the average rainfall and rainfall intensity of the unit. Only the spatial distribution map of the rainfall erosivity factors in certain sections (June 5, 2014) is shown because of space constraints (Figures 7 and 8).



340
341

Figure 7. Spatial distribution map of rainfall erosivity factors (K127-K139+800)



342
343

Figure 8. Spatial distribution of rainfall erosion factor in typical a section of a highway

344 3.2.2 Soil erodibility factor (K)

345 The soil data of a slope in each section were obtained by sampling according to the spatial
346 distribution map of soil types in the study area and by dividing the linear distribution of the soil.
347 The K value was calculated by applying Formula 4 to obtain the soil erodibility factor values of
348 each slope (Sharply and Williams, 1990) (Tables 3 and 4; see supplementary material/appendices).

$$349 \quad K = 0.2 + 0.3e^{[0.0256SAN(1-SIL/100)]} \times \left(\frac{SIL}{CLA + SIL} \right)^{0.3} \times \left[1 - \frac{0.25C}{C + e^{3.72-2.95C}} \right] \times \left[1 - \frac{0.75N_1}{SN_1 + e^{22.9SN_1-5.51}} \right] \quad (4)$$

350 In the formula, SAN, SIL, CLA and C represent sand grains (0.05–2 mm), powder (0.002–
351 0.05 mm), clay (<0.002 mm) and organic carbon content (%), respectively; $SN_1=1-SAN/100$.

352

353 3.2.3 Calculation of topographic factors in natural slope catchments

354 (1) Slope length factor

355 On the basis of the topographic map (1:2000 scale) and highway design of Xinhe Expressway,
356 the slope length and factor of the slope catchment were calculated by using DEM data with 0.5 m
357 spatial resolution generated by ArcGIS. The natural slope catchment was divided into less than 1° ,
358 $1^\circ-3^\circ$, $3^\circ-5^\circ$ and greater than or equal to 5° by using the 'reclassify' tool in ArcGIS. The L factor
359 algorithm of Moore and Burch (1986) was utilised in the operation formulas (Formulas (5) and
360 (6)).

$$361 \quad L = \left(\frac{\lambda}{22.13} \right)^m \quad (5)$$

$$362 \quad \lambda = flowacc \cdot cellsize, \quad (6)$$

363 where L is normalised to the amount of soil erosion along the slope length of 22.13 m, λ is the
364 slope length, $flowacc$ is the total pixel number of water flowing into the pixel that is higher than
365 the pixel and $cellsize$ refers to the DEM resolution size. The value is 0.5 m, and m is the LS factor.
366 Formula (7) is expressed as

$$367 \quad m = \begin{cases} 0.2 & \theta < 1^\circ \\ 0.3 & 1^\circ \leq \theta < 3^\circ \\ 0.4 & 3^\circ \leq \theta < 5^\circ \\ 0.5 & \theta \geq 5^\circ \end{cases} \quad (7)$$

368 where θ is the slope.

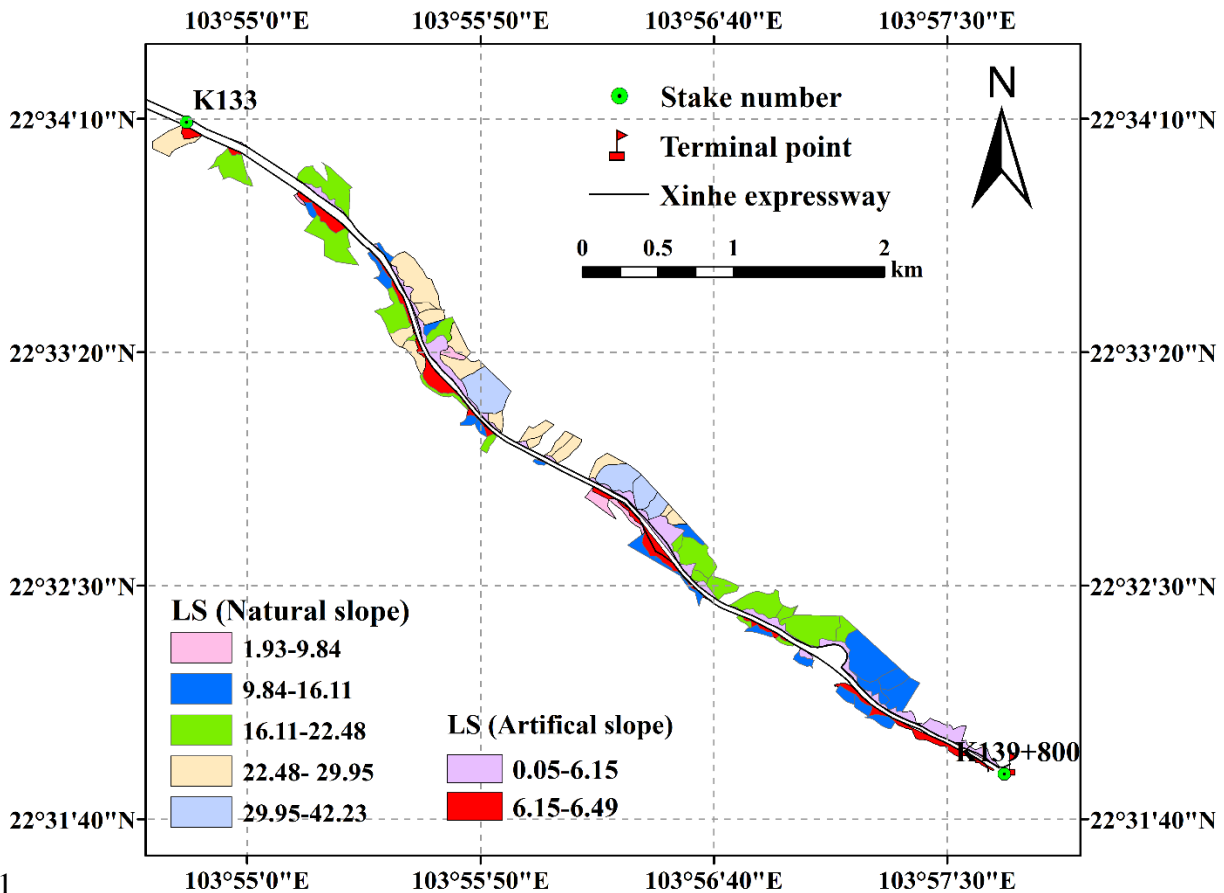
369 (2) Slope factor

370 The S factor was calculated as follows. If the slope was less than 18° , then the formula of
 371 McCool et al. (1987) was used. If the slope was greater than 18° , then the formula of Liu et al.
 372 (1994) was adopted. Formula (8) is expressed as

$$373 \quad S = \begin{cases} 10.8 \cdot \sin \theta + 0.03 & \theta < 9^\circ \\ 16.8 \cdot \sin \theta - 0.05 & 9^\circ \leq \theta < 18^\circ \\ 21.9 \cdot \sin \theta - 0.96 & \theta \geq 18^\circ \end{cases} \quad (8)$$

374 The DEM data were processed by ArcGIS to obtain slope data. The slope values of each
 375 prediction unit were extracted by using the Zonal statistics tool. With the classification tool in
 376 ArcGIS, the slope of the highway catchment of Xinhe was divided into less than 9° , $9-18^\circ$ and
 377 greater than or equal to 18° .

378 The S values of the slope catchments under the three slope grades were calculated by
 379 combining Formula (8) with ArcGIS techniques. The LS values of the slope prediction units are
 380 shown in Figure 9.



381

382

Figure 9. Spatial distribution map of topographic factors (K134–K139)

383 3.2.4 Calculation of topographic factors of artificial slopes

384 (1) Slope length factor

385 The method of Chen Zongwei (2010) was used for the calculation of the *LS* factor of the
386 artificial slopes, and the calculation method for the topographic factors of the artificial slopes of
387 Xinha Expressway was modified. The slope length factor (L_a) was calculated using Formulas (5)
388 and (6). The slope length index (m_a) was measured by conducting a runoff plot experiment and
389 calculated using Formula (9).

390
$$m_a = \log_{\frac{\lambda_1}{\lambda_2}} \frac{A_1}{A_2}, \quad (9)$$

391 where A_1 and A_2 are the soil erosion intensity values of two slopes when the slope lengths are λ_1
392 and λ_2 , respectively (i.e. the specifications of the two slopes are the same except for slope length).
393 The soil erosion amounts under 30 erosion rainfall conditions were monitored in the runoff field
394 of Xiao Xinzhai in Mengzi City in 2014–2015 (Table 5). The m_a value under each rainfall
395 condition was calculated using Formula (9) according to the monitoring value of soil erosion
396 amount. The average value of m_a was 0.32, and it was regarded as the m_a value of the artificial
397 slope length factor (Table 6).

398

399 (2) Slope factor

400 The calculation of the slope factor was based on the method of Chen Zongwei (Chen et al.,
401 2010). Six runoff plots were established in the Xiao Xinzhai runoff field of Mengzi City. Soil
402 erosion intensity under the slope conditions of 1:1.5, 1:1.0 and 9:100 was monitored. Then, the
403 slope factor for the slope condition was obtained using Formula (10).

404
$$S_\theta = \frac{A_\theta}{A}, \quad (10)$$

405 where S_θ represents the slope factor when the slope is θ , A_θ represents the soil erosion intensity
406 when the slope is θ (t/hm²) and A represents the soil erosion intensity when the slope is 9% (t/hm²).
407 The three slope conditions (1:1.5, 1:1.0 and control slope of 9:100) in the soil erosion monitoring
408 experiment were combined with Formula (10) to calculate the slope factor values of the two

409 slopes (1:1.5 and 1:1.0) under 30 rainfall conditions. The average factors of the slopes under the
 410 1:1.5 and 1:1.0 slope conditions were 7.28 and 14.49, respectively (Table 7).

411 After the slope design drawings were digitised by ArcGIS, the slope and length values of each
 412 artificial slope prediction unit were determined according to design specifications. The slope
 413 length value of each artificial slope prediction unit was regarded as the horizontal projection
 414 length of the cement frame. The slope length of the six arris brick revetments was 0. Formulas (5),
 415 (6), (9) and (10), in combination with the slope length factor and m_a and S_θ values, were used to
 416 calculate the value of LS of each artificial slope prediction unit.

417 **Table 7.** Calculation results of the slope factor

Time of the second rainfall	S_{46}	S_{56}
2014.06.05	7.23	14.52
2014.06.07	7.25	14.47
2014.06.17	7.25	14.41
2014.06.28	7.33	14.62
2014.07.01	7.28	14.57
2014.07.13	7.27	14.57
2014.07.20	7.28	14.52
2014.08.02	7.20	14.43
2014.08.12	7.23	14.46
2014.08.26	7.27	14.60
2014.08.29	7.24	14.44
2014.09.02	7.25	14.56
2014.09.04	7.33	14.72
2014.09.17	7.30	14.32
2014.09.20	7.28	14.49

2014.10.05	7.33	14.73
2015.07.04	7.23	14.36
2015.07.15	7.24	14.32
2015.07.24	7.17	14.15
2015.07.28	7.39	14.68
2015.08.13	7.28	14.47
2015.08.19	7.33	14.53
2015.08.26	7.35	14.47
2015.09.03	7.22	14.47
2015.09.12	7.28	14.47
2015.09.17	7.29	14.48
2015.09.25	7.28	14.47
2015.10.03	7.27	14.53
2015.10.08	7.36	14.71
2015.10.12	7.40	14.26
Average	7.28	14.49

418 *Note: S_{xy} represents the slope factor value simultaneously solved by erosion intensity values for monitoring plots*
419 *numbered x and y .*

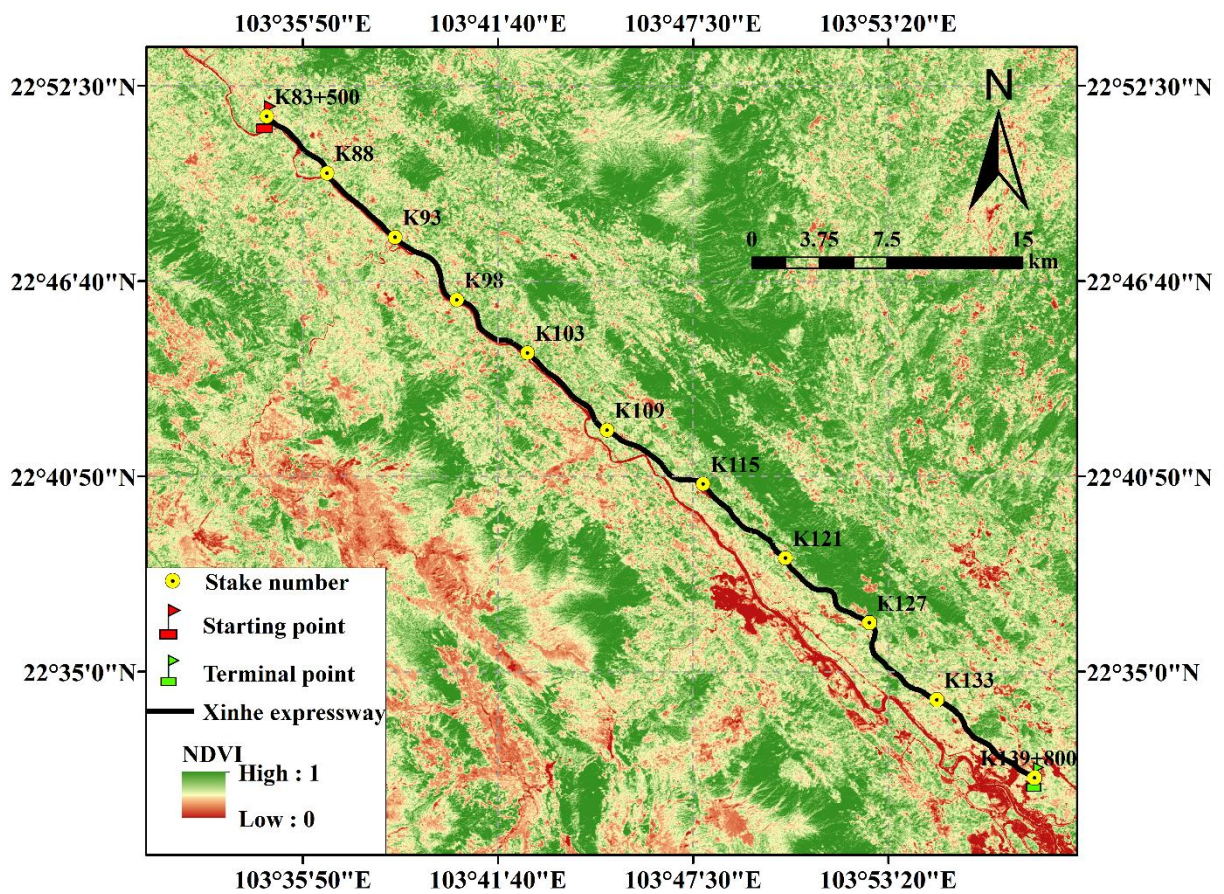
420

421 3.2.5 Cover and management practice factor

422 The C factor after topographic analysis is **vital in** soil loss risk control. In the RUSLE model,
423 the C factor is used to depict the effects of vegetation cover and management practices on the soil
424 erosion rate (Vander-Knijff et al., 2000; Prasannakumar et al., 2011; Alkharabsheh et al., 2013).
425 The C factor is defined as the loss ratio of soils from cropped land under specific conditions to the
426 corresponding loss from clean-tilled and continuous fallow (Wischmeier and Smith, 1978).
427 **Datasets from satellite remote sensing were initially used to assess the C factor due to the various**
428 **land cover patterns with severe spatial and temporal variations mainly at the watershed scale**
429 **(Vander-Knijff et al., 2000; Li et al., 2010; Chen et al., 2011; Alexakis et al., 2013). By taking full**

430 advantage of NDVI data, C was calculated according to the equation of Gutman and Ignatov
 431 (1998) (i.e. Formula (11)). Then, the vegetation coverage data were corrected by examining a
 432 sample plot every 2 km along the study area. The algorithm for calculating f was adopted from the
 433 work of Tan et al. (2005) (i.e. Formula (11)). Finally, accurate vegetation coverage data were
 434 obtained (Figure 10). The C factor map of the soil erosion prediction unit for the slope catchment
 435 area is shown in Figure 11.

436
$$C = 1 - \frac{NDVI - NDVI_{\min}}{NDVI_{\max} - NDVI_{\min}} \quad (11)$$



437
 438

Figure 10. Vegetation coverage along Xinhe Expressway

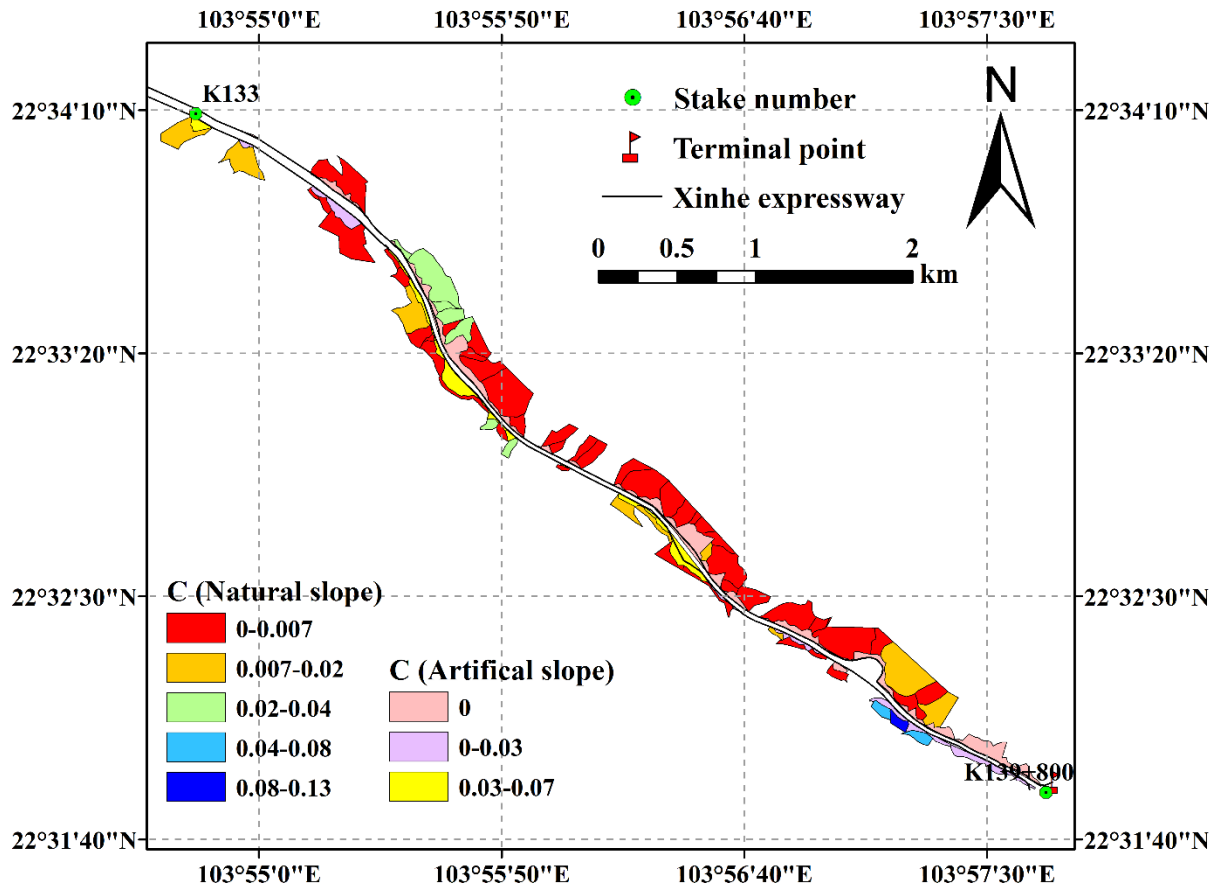


Figure 11. Spatial distribution map of the cover and management practice factor

3.2.6 Soil and water conservation measures

The land use types in the natural slope catchment area were classified as cultivated, forest, construction and difficult lands. Through a field investigation and visual judgment, the water conservation measures of farmland and forestland were identified as contour belt tillage, horizontal terrace and artificial slope catchment area, including cement frame and six arris brick revetments. The P values of the cement frame and the six arris brick revetments, which were determined by using the area ratio method, were 0.85 and 0.4, respectively. The P values of the soil and water conservation measures are shown in Table 8.

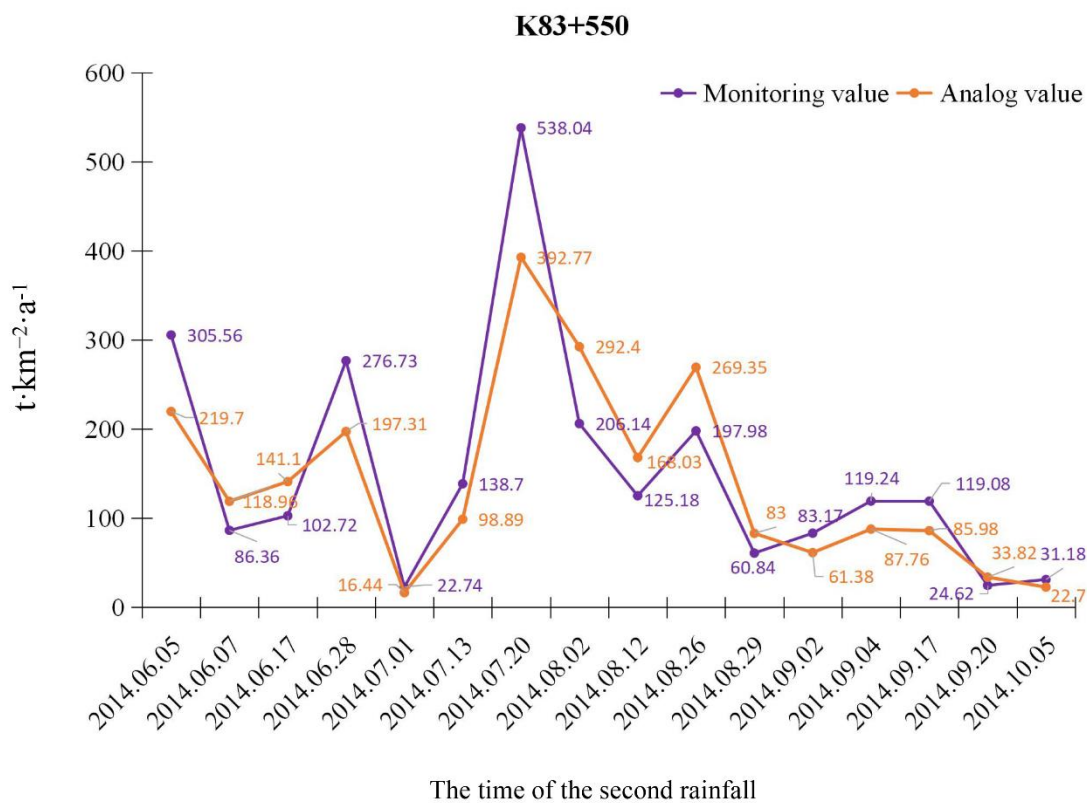
Table 8. P values of different slope types

Slope type	Cement frame	Hexagonal brick	Contour strip tillage	Level bench/terrace	Construction land	Difficult to use land	Others
P	0.85	0.4	0.55	0.03	0	0.2	1

451 **3.3 Validation of model simulation accuracy**

452 Soil erosion in three monitoring areas under 16 erosive rainfall conditions was monitored in
 453 2014. No rainfall occurred in the 24 h before each rainfall event, and the disturbance of antecedent
 454 rainfall on soil erosion on the slopes was excluded. After estimating the historical soil and water
 455 loss of each slope prediction unit, the results were compared with data from the three monitoring
 456 plots along the side slope of Xinde Expressway (Figures 12–14).

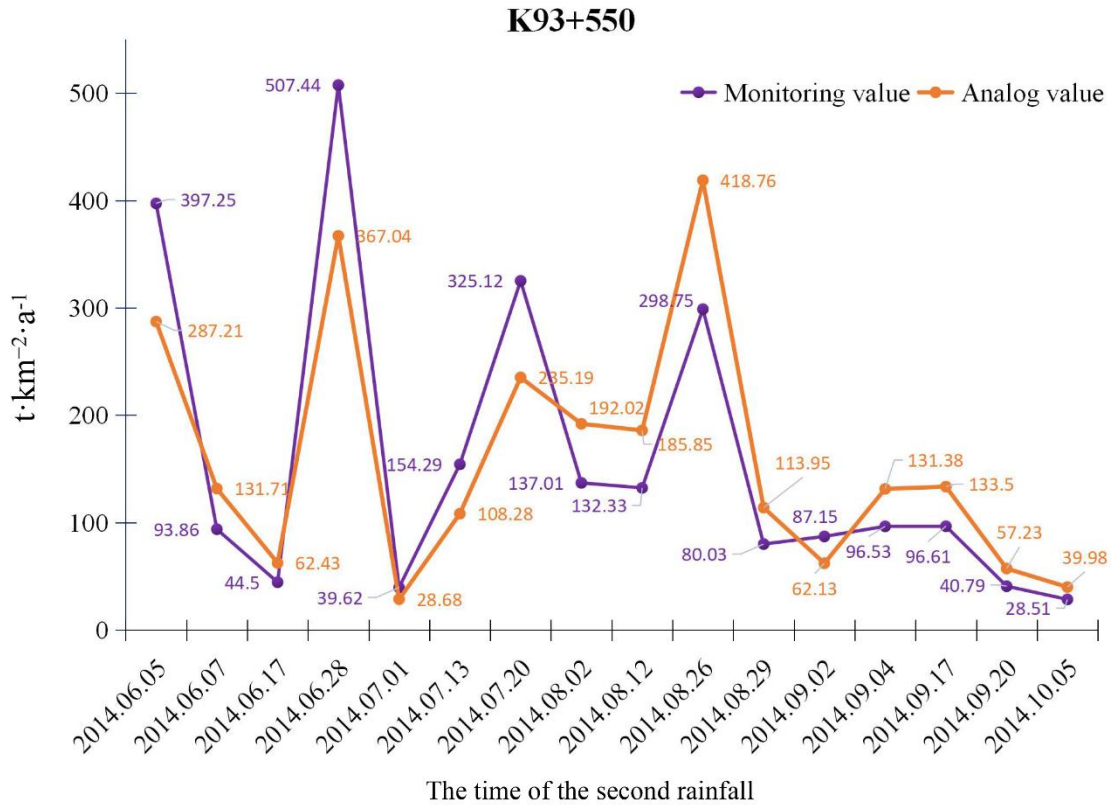
457



458

459

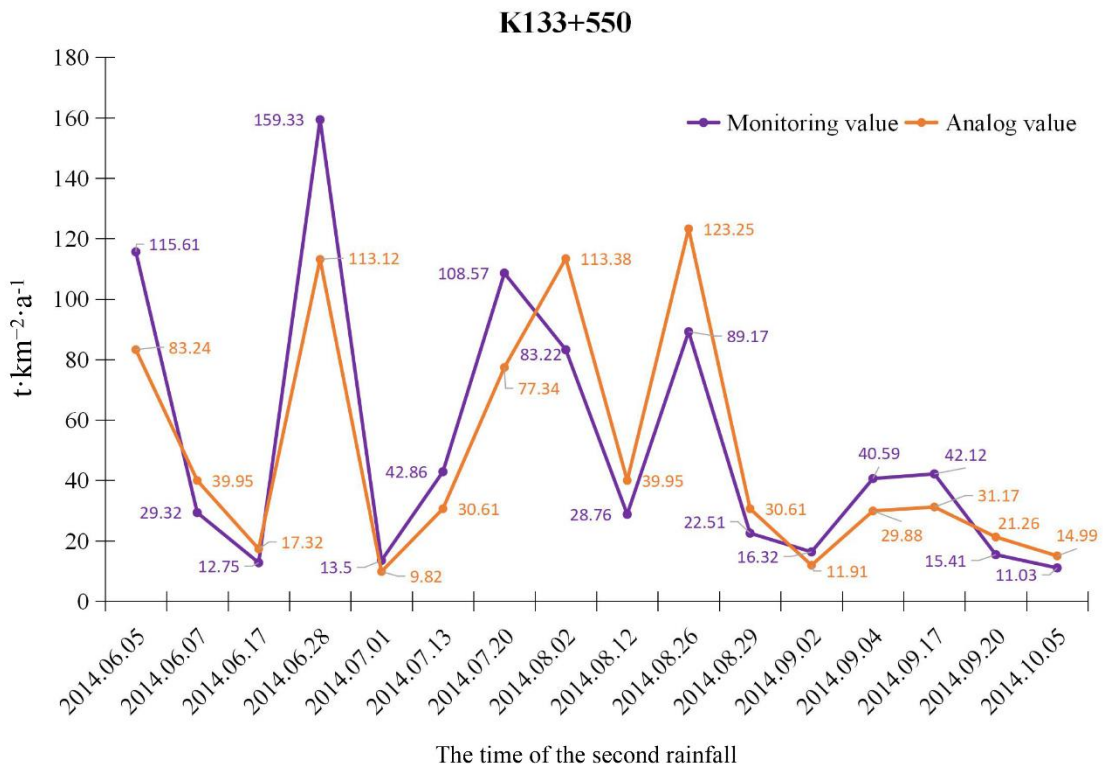
Figure 12. Comparison of model prediction and monitoring results (K83+550)



460

461

Figure 13. Comparison of model prediction and monitoring results (K93+550)



462

463

Figure 14. Comparison of model prediction and monitoring results (K133+550)

464

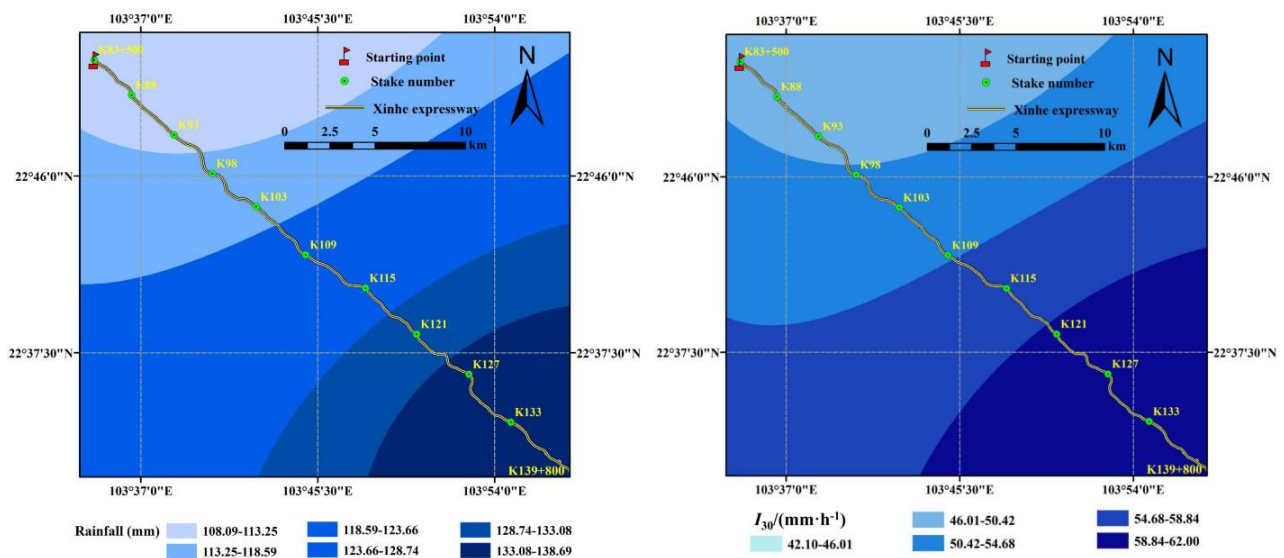
465 The error analysis showed that the absolute errors of the three monitoring areas under the 16
 466 rainfall conditions were 47.15, 52.52 and 16.27 $t \cdot km^{-2} \cdot a^{-1}$, and the overall average absolute error
 467 was 38.65 $t \cdot km^{-2} \cdot a^{-1}$. The average relative errors were 31.80%, 35.49% and 32.26%, and the
 468 overall mean relative error was 31.18%. The root mean square errors were 59.44, 65.6, and 20.95,
 469 all of which were within the acceptable range. The Nash efficiency coefficient of the model was
 470 0.67, which is between 0 and 1, thereby showing that the model's accuracy satisfied the
 471 requirements. The calculation results are shown in Tables 10–12 (see supplementary
 472 material/appendices).

473 The northern and flat terrains of the southern region had a small simulation error because of
 474 the high and low areas of the central region of the terrain, which resulted in a slightly lower
 475 accuracy than that for the southern region. The absolute error of the simulation was large under
 476 heavy rainfall conditions. On the one hand, this result may be caused by the artificial error in
 477 sediment collection in the area. On the other hand, the model itself may be defective.

478

479 3.4 Application of early warning of soil erosion to the mountain expressway

480 The rainfall data and I_{30} values in the 20 years covered by the study were obtained from the
 481 meteorological departments of Mengzi, Pingbian, Jinping and Hekou counties in Yunnan Province.
 482 Rainfall and its intensity were interpolated by co-kriging, which was introduced into the elevation
 483 and geographical position (Figures 15 and 16).



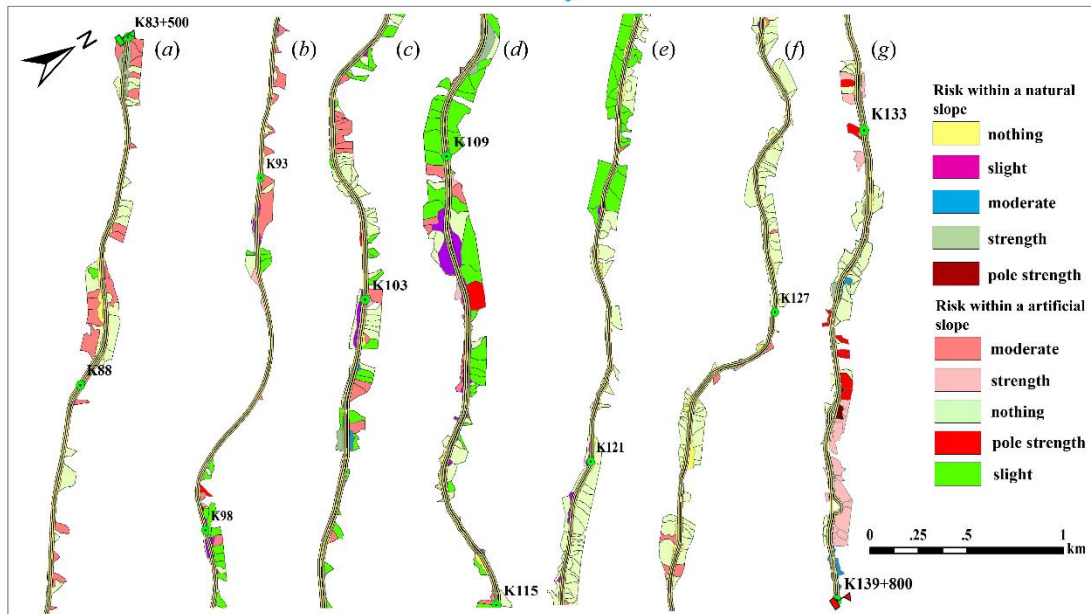
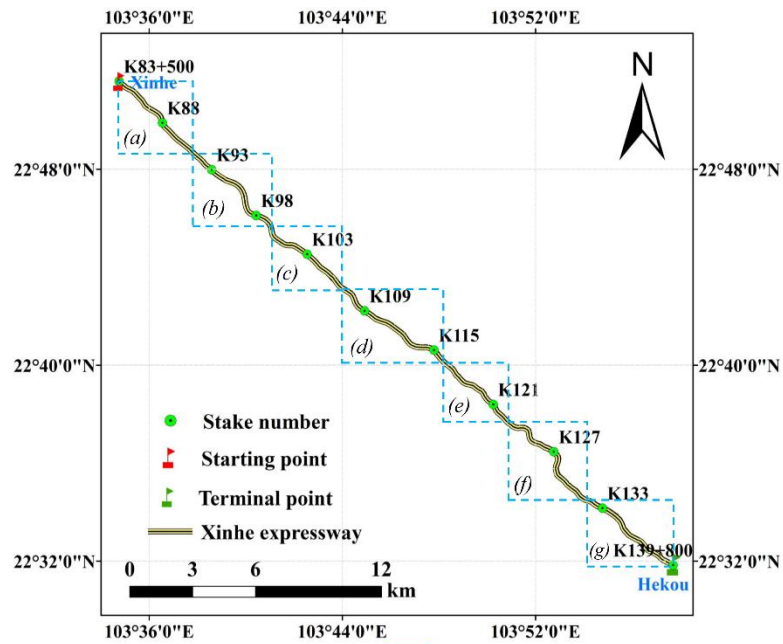
484

485 **Figure 15.** Rainfall interpolation results under 20-year return period

486 **Figure 16.** Rainfall intensity interpolation results under 20-year return period

487 The total soil erosion amount of each prediction unit for the 20-year rainfall data was

488 obtained by simulation according to the classification standards of soil erosion intensity. The
 489 prediction results were classified as ‘no risk’, ‘slight risk’, ‘moderate risk’, ‘high risk’ and
 490 ‘extremely high risk’ (Figure 17).



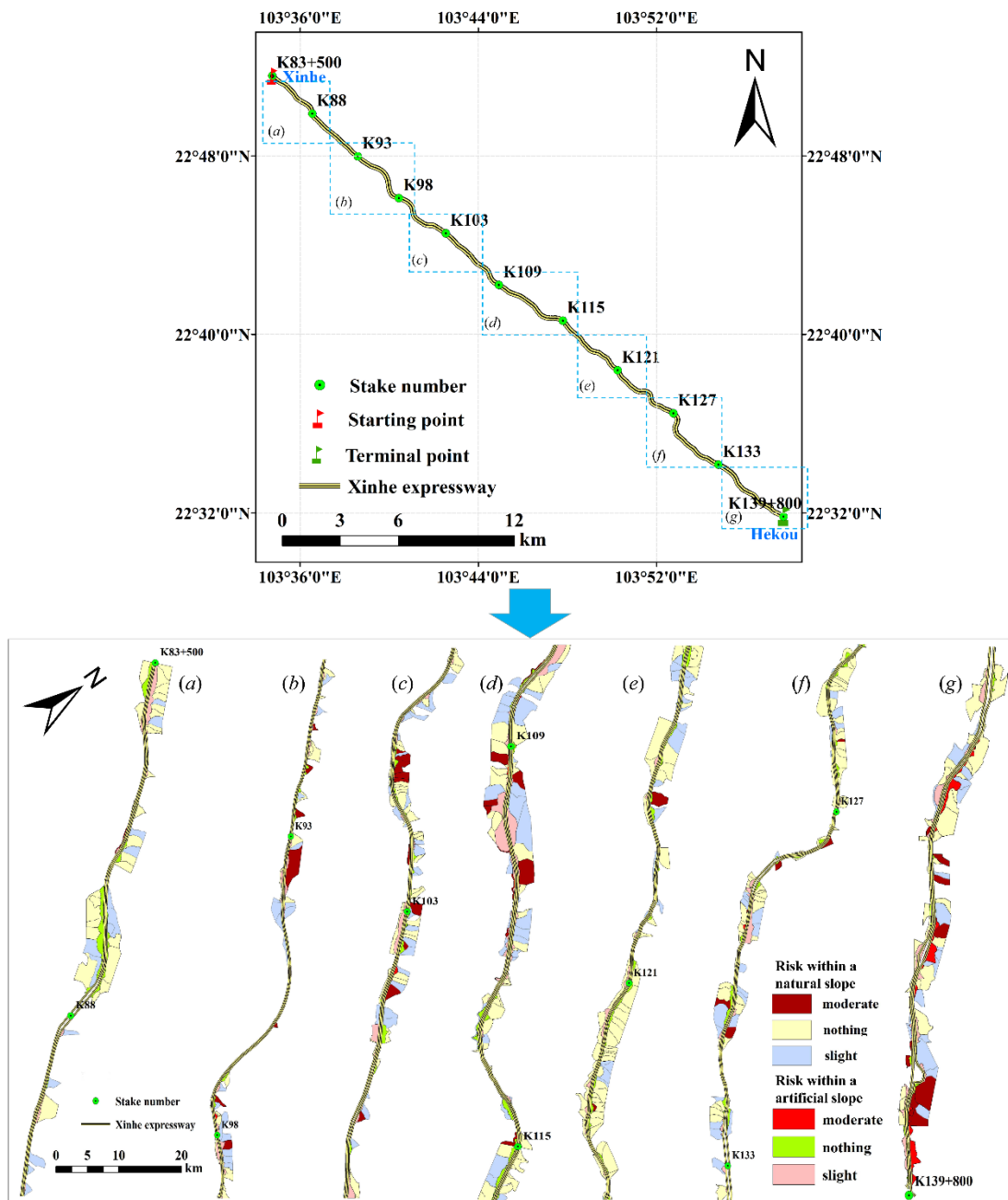
491
 492

Figure 17. Risk analysis of soil and water loss under 20-year rainfall conditions

493 The grading results showed that the percentage of prediction units classified as having low
 494 and mild risks of soil and water loss was 88.60%. Given that the risk of soil erosion is low in these
 495 areas, road traffic safety is not affected. The percentage of prediction units classified as having a
 496 moderate risk was 4.29%. The risk of soil erosion in these areas is relatively low under general
 497 rainfall intensity conditions. However, with high rainfall intensity, a certain scale of soil erosion
 498 disaster could occur. The percentage of prediction units labelled as ‘high risk’ and ‘extremely high

499 risk' was 7.11%. The risk of soil erosion is high in these units. For example, from K134+500 to
 500 K135+500 (1000 m), the average soil erosion amount on both sides of the slope for the 20-year
 501 rainfall amount reached 1757 t·km⁻²·a⁻¹. Even if only a portion of the sediment is deposited on the
 502 road, road safety will still be affected.

503 Similarly, the risk of soil erosion was analysed according to the grading standard of soil and
 504 water loss risk under the 20-year rainfall condition. This analysis was performed by simulating the
 505 soil erosion amount of each prediction unit for the 1-year rainfall amount (Figure 18).



506
 507 **Figure 18.** Risk analysis of soil and water loss for the 1-year rainfall amount

508 The results indicated that the risk percentages of the prediction units for no soil erosion and

509 mild soil erosion were 78.00% and 17.92%, respectively. **Given that the** risk of soil erosion **is** low
510 in these areas, the safety of road traffic **is** not affected. The **risk** percentage of prediction units for
511 mild soil erosion was 6.08%. Therefore, the layout of soil and water conservation measures in
512 these areas should be rationally adjusted. Moreover, **comprehensive management of their slopes**
513 **should be strengthened**, and plant and engineering measures should be applied comprehensively to
514 conserve soil and water in these regions. **Inspections must be reinforced**, and motorists should be
515 reminded to focus on traffic safety during rainy seasons. Most of the artificial slopes covered by
516 the study area are made of six arris brick revetment; that is, the amount of soil erosion is small,
517 and the frame-type cement slope protection against soil erosion is sturdier than those in other areas.
518 Slope protection measures should be rationally adjusted according to **the** predicted results. We
519 may **adopt ecological slope protection technologies to slow** down the roadbed slope **and thus** keep
520 the slope stable. For example, the spraying and planting technology for bolt hanging nets can be
521 used to build a layer of planting matrix that can grow and develop on the weathered rock slope
522 **because** it can resist the porous and stable structure of the scouring. Technologies **for** masonry
523 **wall maintenance** and honeycomb grid revetment protection can also be used. Various **other**
524 technologies can be adopted **to** prevent and control soil erosion, and they can beautify the
525 landscape environment of the road area whilst ensuring road traffic safety.

526

527 **4 Discussion**

528 Slope is the main factor of **the** soil and water loss caused by highways. **Thus, slope is crucial**
529 **for prediction and early warning systems**. A highway slope can be divided into natural and
530 engineering (artificial) slopes, **and the** RUSLE model can be used to predict soil erosion **on** natural
531 slopes. **Disregarding** rainfall erosivity variations, we **found** that the methods of model parameter
532 acquisition **for** literature analysis and **for** comparison **of** areas of the same type **are consistent**
533 (Yang 1999; Yang 2002; Peng et al., 2007; Zhao et al., 2007; Chen et al., 2014; Zhu et al., 2016).
534 **After** comparing the monitoring data with runoff plots, we **discovered** that the error between the
535 predicted value and the monitoring value calculated by the RUSLE model is negligible (Yang
536 1999; Yang 2002; Li et al., 2004). These findings indicate that the prediction results of the model
537 are reliable. In the prediction of erosion **on** engineering (artificial) slopes, previous studies
538 emphasised surface disturbance during construction (He, 2004; Liu et al., 2011; He, 2008; Hu,
539 2016; Zhang et al., 2016; Song et al., 2007) but did not consider soil erosion as a result of the
540 construction. In the process of predicting soil and water loss in engineering slopes by using the
541 RUSLE model, the correction of the conservation support factor (i.e. cement block and
542 hexagonal brick) is often ignored (Zhang, 2011; Morschel et al., 2004; Correa and Cruz, 2010). In
543 addition, most cases use RUSLE modelling to predict the soil erosion **on** highway slopes. Remote
544 sensing is usually based on grid data **and** does not consider catchment units (IsIam et al., 2018;
545 Villarreal et al., 2016; Wu and Yan 2014; Chen et al., 2010).

546 In this study, we analysed the characteristics of soil erosion during expressway construction
547 to improve **several** aspects of previous research. **First, we** divided the highway slope into natural
548 and artificial units and calculated the amount of soil loss from the slope surface to the pavement
549 based on the slope surface catchment unit. **Given that** this approach is more in line with the actual
550 situation than previous methods, the findings of the present study can be popularised. **Second, we**
551 considered the spatial heterogeneity of the linear engineering of an expressway. **The** rainfall factor
552 was spatially interpolated to compensate for the limitations on rainfall data, which were usually
553 used by previous studies. **Third, we** modified the parameters of the artificial slope **through an**
554 actual survey, runoff plot observation and other methods, and the parameters of the artificial slope
555 **were** corrected by referring to the form of the project and the utilised materials.

556

557 **5 Conclusions**

558 The error analysis of the actual observation data showed that the overall average absolute
559 error of each monitoring area was $38.65 \text{ t}\cdot\text{km}^{-2}\cdot\text{a}^{-1}$, the average relative error was 31.18%, the
560 root mean square error was between 20.95 and 65.64 and the Nash efficiency coefficient was 0.67.
561 **The method of soil and water loss prediction adopted in this work generally has a smaller error**
562 **and higher prediction accuracy than other models**, and it can satisfy prediction requirements. **The**
563 **risk grades of soil and water loss along the slope of Xinhe Expressway were divided into 20- and**
564 **1-year rainfall conditions based on simulated predictions. The results showed that the percentage**
565 **of slope areas with high and extremely high risks was 7.11%**. These areas are mainly located in
566 the K109+500–K110+500 and K133–K139+800 sections. Therefore, relevant departments should
567 strengthen disaster prevention and reduction efforts and corresponding water and soil conservation
568 initiatives in these areas.

569

570 **6 Acknowledgment**

571 This study was jointly supported by the Yunnan Provincial Communications Department Project
572 (2012-272-(1)) and the Yunnan Provincial Science and Technology Commission Project
573 (2014RA074).

574

575 **7 References**

576 Alexakis, D., Diofantos, G., Hadjimitsis, A.: Integrated use of remote sensing, GIS and
577 precipitation data for the assessment of soil erosion rate in the catchment area of “Yialias” in
578 Cyprus. *Atmospheric Research*, 131, 108-124, 2013.

579 Alkharabsheh, M.M., Alexandridis, T.K., Bilasb, G., Misopolinos, N.: Impact of land cover change
580 on soil erosion hazard in northern Jordan using remote sensing and GIS. *Four decades of*

- 581 progress in monitoring and modeling of processes in the soil-plant-atmosphere system:
582 applications and challenges. *Procedia Environmental Science*, 19, 912-921, 2013.
- 583 Angulomartínez, M., and Beguería, S.: Estimating rainfall erosivity from daily precipitation
584 records: a comparison among methods using data from the ebro basin (NE Spain). *Journal of*
585 *Hydrology*, 379(1): 111-121, 2009.
- 586 Bakr, N., Weindorf, D. C., Zhu, Y. D., Arceneaux, A. E., Selim, H. M.: Evaluation of
587 compost/mulch as highway embankment erosion control in Louisiana at the plotscale. *Journal*
588 *of Hydrology*, s 468-469(6): 257-267, 2012.
- 589 Bosco, C., De Rigo, D., Dewitte, O., Poesen, J., and Panagos, P.: Modelling soil erosion at
590 European scale: towards harmonization and reproducibility. *Natural Hazards & Earth System*
591 *Sciences*, 2(4), 2639-2680, 2015.
- 592 Cai, C. F., Ding, S. W., Shi, Z. H., Huang, L., Zhang, G. Y.: Study of Applying USLE and
593 Geographical Information System IDRISI to Predict Soil Erosion in Small Watershed.
594 *Journal of Soil and Water Conservation*. 14(2): 19-24, 2000.
- 595 Chen, B. H.: The study on multivariate spatial interpolation method of precipitation in
596 mountainous areas. Beijing Forestry University, 2016 (in Chinese).
- 597 Chen, F., Zeng, M. G., and Zhou, Z. H.: Evaluation for Ecological Benefits of Greening on
598 Expressways in Mountainous Area. *Technology of Highway and Transport*, 1:139-143, 2015
599 (in Chinese).
- 600 Chen, S. X., Yang, X. H., Xiao, L. L., Cai, Y. H.: Study of Soil Erosion in the Southern Hillside
601 Area of China Based on RUSLE Model. *Resources Science*, 36(6): 1288-1297, 2014 (in
602 Chinese).
- 603 Chen, T., Niu, R. Q., Li, P. X., Zhang, L. P., Du, B.: Regional soil erosion risk mapping using
604 RUSLE, GIS, and remote sensing: a case study in Miyun watershed, North China.
605 *Environmental Earth Sciences*, 63(3), 533-541, 2011.
- 606 Chen, Y. J., Sun, K. M., and Zhao, Y.: Experiment on the effect of rule caused by slope angle on
607 sand and runoff under the condition of ecological protected slope. *Journal of Water Resources*
608 *& Water Engineering*, 21(4):55-59, 2010 (in Chinese).
- 609 Chen, Z. W., He, F., and Wang, J. J.: Revises of Terrain Factors of Roadbed Side Slope in
610 Universal Soil Loss Equation. *HIGHWAY*, 12:180-185, 2010 (in Chinese).
- 611 Chen, Z. W., He, F., and Wang, J. J.: Revises of Terrain Factors of Roadbed Side Slope in
612 Universal Soil Loss Equation. *HIGHWAY*, 12:180-185, 2010 (in Chinese)
- 613 Chen, Z. W., He, F., Wang, J. J.: Revises of Terrain Factor of Roadbed Side Slope in Universal
614 Soil Loss Equation. *HIGHWAY*, (12):180-185, 2010 (in Chinese).
- 615 Correa, C. M. C., Cruz, J.: Real and estimative erosion through RUSLE from forest roads in
616 undulated at heavily undulated relief. *Revista Árvore*, 34(4): 587-595, 2010.
- 617 Cunha, E. R. D., Bacani, V. M., Panachuki, E.: Modeling soil erosion using RUSLE and GIS in a
618 watershed occupied by rural settlement in the Brazilian Cerrado. *Natural Hazards*, 85, 1-18,
619 2017.
- 620 Dong, H., Zeng, H.: Discussion on the current situation and the future of China highway

- 621 construction. *Technology & Economy in Areas of Communication (TEAC)*, 5(3):17-18, 2003
622 (in Chinese).
- 623 Fei, X. H., Song, Q. H., Zhang, Y. P., Liu, Y. T., Sha, L. Q., Yu, G. R., Zhang, L. M., Duan, C. Q.,
624 Deng, Y., Wu, C. S., Lu, Z. Y., Luo, K., Chen, A. G., Xu, K., Liu, W. W., Huang, H., Jin, Y. Q.,
625 Zhou, R. W., Grace, J.: Carbon exchanges and their responses to temperature and
626 precipitation in forest ecosystems in Yunnan, Southwest China. *Science of The Total
627 Environment*, 616: 824-840, 2017.
- 628 Feng, Q., and Zhao, W. W.: The study on cover-management factor in USLE and RUSLE: a
629 review. *ACTA ECOLOGICA SINICA*, 34(16):4461-4472, 2014 (in Chinese).
- 630 Fenta, A. A., Yasuda, H., Shimizu, K., Haregeweyn, N., and Negussie, A.: Dynamics of Soil
631 Erosion as Influenced by Watershed Management Practices: A Case Study of the Agula
632 Watershed in the Semi-Arid Highlands of Northern Ethiopia. *Environmental Management*,
633 58(5): 1-17, 2016.
- 634 Foster, G. R., Weesies, G. A., McCool, D. K., Joder, D. C., Renard, K. G.: Revised Universal Soil
635 Loss Equation User's Manual. Gov. Print. Office, Washington D.C. (48p), 1999.
- 636 Gong, J., and Yang, P.: Study on the Layout of Soil and Water Conservation Monitoring Sites
637 during the Construction of Mountain Highways-Case Study of Enlai, Enqian Highway.
638 *Subtropical Soil and Water Conservation*, 28(1):9-11, 2016 (in Chinese).
- 639 He, F.: Prediction of soil erosion in foundation slope of South Hubei Road Based on RUSLE.
640 Beijing Normal University, 2008 (in Chinese).
- 641 He, X. W.: Study on prediction of soil erosion in Road area. Beijing Normal University, 2004 (in
642 Chinese).
- 643 Hu, L.: Study on development and mechanism of water Erosion and Ecological water erosion
644 control technology of Highway slope in Cold Region. Xi'an University of technology, 2016
645 (in Chinese).
- 646 Islam, M. R., Wan, Z. W. J., Lai, S. H., Osman, N., Din, M. A. M., Zuki, F. M.: Soil erosion
647 assessment on hillslope of GCE using RUSLE model. *Journal of Earth System Science*,
648 127(4): 50, 2018.
- 649 Jia, Y. H., Dai, D. C., Liu, Y.: Performance Analyse and Evaluation of Freeway in China.
650 *JOURNAL OF BEIJING JIAOTONG UNIVERSITY*, 29(6):1-5, 2005 (in Chinese)
- 651 Jia, Z. R., Guo, and Z. Y.: Quantifying Evaluation Approach to Highway Soil Bioengineering.
652 *Research of Soil and Water Conservation*, 15(2):260-262, 2008 (in Chinese).
- 653 Jiang, M., Pan, X. Y., Nie, W. T.: Preliminary analysis of prevention and control of soil and water
654 loss in expressway project construction. *Yangtze River*, 48(12):61-64, 2017 (in Chinese).
- 655 Kateb, H. E., Zhang, H. F., Zhang, P. C., Mosandl, R. Soil erosion and surface runoff on different
656 vegetation covers and slope gradients: A field experiment in Southern Shaanxi Province,
657 China. *Catena*, 105(5): 1-10, 2013.
- 658 Kateb, H. E., Zhang, H. F., Zhang, P. C., Mosandl, R. Soil erosion and surface runoff on different
659 vegetation covers and slope gradients: A field experiment in Southern Shaanxi Province,
660 China. *Catena*, 105(5): 1-10, 2013.
- 661 Kinnell, P. I. A.: Applying the RUSLE and the USLE-M on hillslopes where runoff production

662 during an erosion event is spatially variable. *Journal of Hydrology*, 519:3328-3337, 2014.

663 Li, H., Chen, X. L., Kyoung, J. L., Cai, X. B., Myung S.: Assessment of soil erosion and sediment

664 Li, J. G., Dao, H. Y., Zhang, L., Zhang, H. K.: Soil and Water Loss Monitoring in the Dianchi
665 Watershed. *Research of Soil and Water Conservation*, 11(2): 75-77, 2004 (in Chinese).

666 Li, Y., Qi S., Cheng, B. H., Ma, J. M., Ma, C., Qiu, Y. D., Chen, Q. Y.: A Study on Factors of
667 Space-time Distributions of Precipitation in Ailao Mountain Area and Comparison of
668 Interpolation Methods. *EARTH AND ENVIRONMENT*, 45(6): 600-610 (in Chinese)

669 Lin, H. L., Zheng, S. T., and Wang, X. L.: Soil erosion assessment based on the RUSLE model in
670 the Three-Rivers Headwaters area, Qinghai-Tibetan Plateau, China. *ACTA
671 PRATACULTURAE SINICA*, 26(7):11-22, 2017 (in Chinese)

672 Liu, B. Y., Nearing, M. A., Shi, P. J., and Jia, Z. W.: Slope length effects on soil loss for steep
673 slopes. *Soil Science Society of America Journal* 64(5): 1759-1763, 2000.

674 Liu, J. T., Zhang, J. B.: Interpolation analysis of the spatial distribution of precipitation in
675 mountain area. *Journal of Irrigation & Drainage*, 25:34-38, 2006 (in Chinese)

676 Liu, S. L., Zhang, Z. L., Zhao, Q. H., Deng, L., Dong, S. K.: Effects of Road on Landscape Pattern
677 and Soil Erosion: A Case Study of Fengqing County, Southwest China. *Chinese Journal of
678 Soil Science*, 42(1): 169-173, 2011 (in Chinese).

679 Liu, W. Y.: Preliminary Study on *R* Index of Zhaotong Basin. *Yunnan Forestry Science and
680 Technology*, (2):24-26, 1999 (in Chinese)

681 Liu, X. Y.: Study on the slope stability and its rheological influence in Mountain highway. Central
682 South University, 2013 (in Chinese).

683 Liu, Z. Y., Zhang, X., Fang, R. H. Analysis of spatial interpolation methods to precipitation in
684 Yulin based on DEM. *Journal of Northwest A&F University (Nat. Sci. Ed.)*, 38:227-234,
685 2010 (in Chinese)

686 Mccool, D. K., Brown, L. C., Foster, G. R., Mutchler, C. K., and Meyer, L. D.: Revised slope
687 steepness factor for the universal soil loss equation. *Transactions of the ASAE-American
688 Society of Agricultural Engineers (USA)*, 30(5): 1387-1396, 1987.

689 Millward, A. A., and Mersey, J. E.: Adapting the rusle to model soil erosion potential in a
690 mountainous tropical watershed. *Catena* 38(2):109-129, 1999.

691 Molla, T., and Sisheber, B.: Estimating soil erosion risk and evaluating erosion control measures
692 for soil conservation planning at Koga watershed in the highlands of Ethiopia. *Solid Earth*, 8,
693 1-23, 2017

694 Moore, I. D., and Burch, G. J.: Physical basis of the length-slope factor in the universal soil loss
695 equation. *Soil Science Society of America Journal*, 50(5): 1294-1298, 1986.

696 Mori, A., Subramanian, S. S., Ishikawa, T., Komatsu, M. A Case Study of a Cut Slope Failure
697 Influenced by Snowmelt and Rainfall. *Procedia Engineering*, 189: 533-538, 2017.

698 Mori, A., Subramanian, S. S., Ishikawa, T., Komatsu, M. A Case Study of a Cut Slope Failure
699 Influenced by Snowmelt and Rainfall. *Procedia Engineering*, 189: 533-538, 2017.

700 Morschel, J., Fox, D. M., & Bruno, J. F.: Limiting sediment deposition on roadways: topographic
701 controls on vulnerable roads and cost analysis of planting grass buffer strips. *Environmental*

- 702 Science & Policy, 7(1): 39-45, 2004.
- 703 Mountain Region of Yunnan Province. SCIENTIA GEOGRAPHICA SINICA, 19(3):265-270,
704 1999 (in Chinese)
- 705 Panagos, P., Ballabio, C., Borrelli, P., Meusburger, K., Klik, A., Rouseva, S., Tadić, M.P.,
706 Michaelides, S., Hrabalíková, M., Olsen, P., Aalto, J., Lakatos, M., Rymaszewicz, A.,
707 Dumitrescu, A., Beguería, S., Alewell, C.: Rainfall erosivity in Europe. Science of the Total
708 Environment, 511:801-814, 2015.
- 709 Panagos, P., Borrelli, P., Meusburger, K., Yu, B., Klik, A., Lim, K.J., Yang, J.E., Ni, J., Miao, C.,
710 Chattopadhyay, N., Sadeghi, S.H., Hazbavi, Z., Zabihi, M., Larionov, G.A., Krasnov, S.F.,
711 Gorobets, A.V., Levi, Y., Erpul, G., Birkel, C., Hoyos, N., Naipal, V., Oliveira, P.T.S., Bonilla,
712 C.A., Meddi, M., Nel, W., Al Dashti, H., Boni, M., Diodato, N., Van Oost, K., Nearing, M.,
713 Ballabio, C. Global rainfall erosivity assessment based on high-temporal resolution rainfall
714 records. Scientific Reports, 7(1): 4175, 2017.
- 715 Panagos, P., Standardi, G., Borrelli, P., Lugato, E., Montanarella, L., Bosello, F.: Cost of
716 agricultural productivity loss due to soil erosion in the European union: from direct cost
717 evaluation approaches to the use of macroeconomic models. Land Degradation &
718 Development. 2018.
- 719 Panos, P., Cristiano, B., Pasquale, B., Katrin, M., Andreas, K., Svetla, R., Melita, P. T., Silas, M.,
720 Michaela, H., Preben, O., Juha, A., Mónica, L., Anna, R., Alexandru, D., Santiago, B., and
721 Christine, A.: Rainfall erosivity in Europe. Science of the Total Environment, 511: 801, 2015.
- 722 Peng, J., Li, D. D., Zhang, Y. Q.: Analysis of Spatial Characteristics of Soil Erosion in Mountain
723 Areas of Northwestern Yunnan Based on GIS and RUSLE. Journal of mountain science,
724 25(5): 548-556, 2007 (in Chinese).
- 725 Prasannakumar, R., Shiny, N., Geetha, H., Vijith, H.: Spatial prediction of soil erosion risk by
726 remote sensing, GIS and RUSLE approach: a case study of Siruvani river watershed in
727 Attapady valley, Kerala, India. Environmental Earth Science, 965-972, 2011.
- 728 Renard, K. G., Foster, G. R., Weesies, G. A., Mccool, D. K., and Yoder, D. C.: Predicting soil
729 erosion by water: a guide to conservation planning with the revised universal soil loss
730 equation (RUSLE). Agriculture Handbook, 1997.
- 731 Renard, K. G., Foster, G. R., Weesies, G. A., McCool, D. K., Yoder, D. C.: Predicting soil erosion
732 by water-a guide to conservation planning with the Revised Universal Soil Loss Equation
733 (RUSLE). United States Department of Agriculture, Agricultural Research Service (USDA-
734 ARS) Handbook No.703. United States Government Printing Office: Washington, DC. 1997.
- 735 Rick, D., Van, R., Matthew, E. H., and Robert J. H.: Estimating the LS Factor for RUSLE through
736 Iterative Slope Length Processing of Digital Elevation Data within ArcInfo Grid. Cartography,
737 30(1): 27-35, 2001.
- 738 Shamshad, A., Azhari, M. N., Isa, M. H., Hussin, W. M. A. W., and Parida, B. P.: Development of
739 an appropriate procedure for estimation of RUSLE EI₃₀ index and preparation of erosivity
740 maps for Pulau Penang in Peninsular Malaysia. Catena, 72(3): 423-432, 2008.
- 741 Sharpley, A. N., and Williams, J. R.: EPIC-erosion/productivity impact calculator: 2. User manual.
742 Technical Bulletin-United States Department of Agriculture, 4(4): 206-207, 1990.

- 743 Shi, Z. H., Cai, C. F., Ding, S. W., Wang, T. W., and Chow, T. L.: Soil conservation planning at the
744 small watershed level using RUSLE with GIS: a case study in the three gorge area of china.
745 *Catena*, 55(1): 33-48, 2004.
- 746 Shu, Z. Y., Wang, J. Y., Gong, W., Lv, X. N., Yan, S. Y., Cai, Y., Zhao, C. P.: Effects of compound
747 management in citrus orchard on soil micro-aggregate fractal features and soil physical and
748 chemical properties. *Journal of Nanjing Forestry University (Natural Sciences Edition)*, 41(5):
749 92-98, 2017.
- 750 Silburn, D. M.: Hillslope runoff and erosion on duplex soils in grazing lands in semi-arid central
751 Queensland. III. USLE erodibility (K factors) and cover-soil loss relationships. *Soil Research*,
752 49(49): 127-134, 2011.
- 753 Soil and Water Conservation Society. RUSLE user's guide. Soil and Water Cons. Soc. Ankeny, IA.
754 164pp, 1993.
- 755 Song, F. L., Ma, Y. H., Zhang, C. X., Yu, H. M., Hu, H. X., He, J. L., Huang, J. Y.: Research
756 progress on greening substrate material of ecological protection of expressway-side slope.
757 *Science of Soil and Water Conservation*, 6:57-61, 2008 (in Chinese).
- 758 Song, X. Q., Zhang, C. Y., Liu, J.: Formation of Soil and Water Loss and Its Characteristics in
759 Development and Construction Projects. *Bulletin of Soil and Water Conservation*, 27(5): 108-
760 113, 2007 (in Chinese).
- 761 Stanchi, S., Freppaz, M., Ceaglio, E., Maggioni, M., Meusburger, K., & Alewell, C., and Zanini,
762 E.: Soil erosion in an avalanche release site (Valle d'Aosta: Italy): towards a winter factor for
763 RUSLE in the Alps. *Natural Hazards & Earth System Sciences*, 14(7), 255-440, 2014.
- 764 Tan, B. X., Li, Z. Y., Wang, Y. H., Yu, P. T., Liu, L. B.: Estimation of Vegetation Coverage and
765 Analysis of Soil Erosion Using Remote Sensing Data for Guishuihe Drainage Basin. *Remote
766 sensing technology and application*. 20 (2): 215-220, 2005.
- 767 Tan, S. H., and Wang, Y. M.: Research Progress and Thinking of Bioengineering Techniques for
768 Slope Protection in Expressway. *Research of Soil and Water Conservation*, 11(3):81-84, 2004
769 (in Chinese).
- 770 Taye, G., Vanmaercke, M., Poesen, J., Wesemael, B. V., Tesfaye, S., Teka, D., et al.: Determining
771 RUSLE P-and C-factors for stone bunds and trenches in rangeland and cropland, North
772 Ethiopia. *Land Degradation & Development*, 29(5), 2017.
- 773 Toy, T. J., Foster, G. R., Renard, K. G.: *Soil Erosion: Processes, Prediction, Measurement, and
774 Control*. 2002
- 775 Tresch, S., Meusburger, K., and Alewell, C.: Influence of slope steepness on soil erosion
776 modelling with RUSLE, measured with rainfall simulations on subalpine slopes. *Bulletin of
777 Hokkaido Prefectural Agricultural Experiment Stations*, 1995.
- 778 Vander-Knijff, J.M., Jones, R.J.A., Montanarella, L.: *Soil Erosion Risk Assessment in Europe
779 EUR 19044 EN*. Office for Official Publications of the European Communities, Luxembourg.
780 34, 2000.
- 781 Villarreal, M. L., Webb, R. H., Norman, L. M., Psillas, J. L., Rosenberg, A. S., Carmichael, S.:
782 Modeling landscape-scale erosion potential related to vehicle disturbances along the USA-
783 Mexico border. *Land Degradation & Development*, 27(4): 1106-1121, 2016.

- 784 Wang, C. J.: Regional Impaction and Evolution of Express Way Networks in China. PROGRESS
785 IN GEOGRAPHY, 25(6):126-137, 2006 (in Chinese)
- 786 Wang, H. J., Yang, Y., and Wang, W. J.: Prediction of Soil Loss Quantity on Side Slope of Freeway
787 Construction: Amendments to Main Parameters of USLE. Journal of Wuhan University of
788 Technology (Transporatation Science & Engineering), 29(1):12-15, 2005 (in Chinese).
- 789 Wang, K., and Gao, Z. L.: Analysis of Bioengineering Technology for Slope Protection of
790 Expressway: Taking Expressway from Ankang to the Border of Shaanxi and Hubei as an
791 Example. Ecological Economy, 31(5):155-159, 2015 (in Chinese).
- 792 Wang, L. H., Ma, B., and Wu, F. Q.: Effects of wheat stubble on runoff, infiltration, and erosion of
793 farmland on the Loess Plateau, China, subjected to simulated rainfall. Solid Earth, 8(2), 1-28,
794 2017.
- 795 Wang, W. Z., and Jiao, J. Y.: Qutantitative Evaluation on Factors Influencing Soil Erosion in China.
796 Bulletin of Soil and Water Conservation, (st):1-20, 1996 (in Chinese).
- 797 Wang, W. Z., and Zhang, X. K.: Distribution of Rainfall Erosivity *R* Value in China. Journal of soil
798 erosion and soil conservation, 2(1): 7-18, 1995.
- 799 Wang, W. Z., Jiao, J. Y., Hao, X. P., Zhang, X. K., Lu, X. Q., Chen, F. Y., Wu, S. Y.: Study on
800 Rainfall Erosivity in China. Journal of Soil and Water Conservation, (4):7-18, 1995 (in
801 Chinese)
- 802 Wischmeier, W.H., Smith, D.D.: Predicting rainfall erosion losses: a guide to conservation
803 planning. In: USDA, Agriculture Handbook No. 537, Washington, DC, 1978.
- 804 Wischmerie, W. H., and Smith, D. D.: Predicting rainfall-erosion losses from cropland east of the
805 rocky mountains: a guide to conservation planning, 1965.
- 806 Wu, Y. L., Yan, L. J.: Impact of road on soil erosion risk pattern based on RUSLE and GIS: a case
807 study of Hangjinqi highway, Zhuji section. ACTA ECOLOGICA SINICA, 34(19):5659-5669,
808 2014 (in Chinese).
- 809 Xiao, P. Q., Shi, X. J., Chen, J. N., Wu, Q., Yang, J. F., Yang, C. X., and Wang, C. G.:
810 Experimental Study on Protecting Speedway Slope Under Rainfall and Flow Scouring.
811 Bulletin of Soil and Water Conservation, 24(1):16-18, 2004 (in Chinese).
- 812 Xu, X. L., Liu, W., Kong, Y. P., Zhang, K. L., Yu, B. F., Chen, J. D.: Runoff and water erosion on
813 road side-slopes: Effects of rainfall characteristics and slope length. Transportation Research
814 Part D: Transport and Environment, 14(7): 497-501, 2009.
- 815 Yang, X.: Deriving rusle cover factor from time-series fractional vegetation cover for hillslope
816 erosion modelling in new south wales. Soil Research, 52(52): 253-261, 2014.
- 817 Yang, Y. C., Wang, M. Z., Xu, Y. Y., Wang, P. C., and Song, Z. P.: Prediction of Soil Erosion on
818 Embankment Slope of Qinhuangdao-Shenyang Special Line for Passenger Trains. Journal of
819 Soil and Water Conservation, 15(2):14-16, 2001(in Chinese).
- 820 Yang, Y., and Wang, K.: Discussions on the Side Slope Protection System For Expressway.
821 Industrial Safety and Environmental Protection, 32(1):47-49, 2006 (in Chinese).
- 822 Yang, Z. S.: A Study on Erosive Force of Rainfall on Sloping Cultivated Land in the Northeast
- 823 Yang, Z. S.: Study on Soil Loss Equation in Jinsha River Basin of Yunnan Province. Journal of
824 mountain science, 20: 3-11, 2002 (in Chinese).

- 825 Yang, Z. S.: Study on Soil Loss Equation of Cultivated Slope Land in Northeast Mountain Region
826 of Yunnan Province. *Bulletin of Soil and Water Conservation*, (1): 1-9, 1999 (in Chinese).
- 827 yield in Liao watershed, Jiangxi Province, China, using USLE, GIS, and RS. *Journal of Earth*
828 *Science* 2 (6), 941-953, 2010
- 829 Yoder, D. C., Foster, G. R., Renard, K. G., Weesies, G. A., and McCool, D. K.: C-factor calculations
830 in RUSLE. American Society of Agricultural Engineers. Meeting (USA), 1993.
- 831 Yuan, C., Yu, Q. H., You, Y. H., Guo, L.: Deformation mechanism of an expressway embankment
832 in warm and high ice content permafrost regions. *Applied Thermal Engineering* 121: 1032-
833 1039, 2017.
- 834 Yuan, C., Yu, Q. H., You, Y. H., Guo, L.: Deformation mechanism of an expressway embankment
835 in warm and high ice content permafrost regions. *Applied Thermal Engineering* 121: 1032-
836 1039, 2017.
- 837 Yuan, J. P.: Preliminary Study on Grade Scale of Soil Erosion Intensity. *Bulletin of Soil and Water*
838 *Conservation*, 19(6):54-57, 1999 (in Chinese).
- 839 Zeng, C., Wang, S. J., Bai, X. Y., Li, Y. B., Tian, Y. C., Li, Y., Wu, L. H., and Luo, G. J. : Soil
840 erosion evolution and spatial correlation analysis in a typical karst geomorphology using
841 RUSLE with GIS. *Solid Earth*, 8(4), 1-26, 2017.
- 842 Zerihun, M., Mohammedyasin, M. S., Sewnet, D., Adem, A. A., & Lakew, M.: Assessment of soil
843 erosion using RUSLE, GIS and remote sensing in NW Ethiopia. *Geoderma Regional*, 12: 83-
844 90, 2018.
- 845 Zerihun, M., Mohammedyasin, M. S., Sewnet, D., Adem, A. A., Lakew, M.: Assessment of soil
846 erosion using RUSLE, GIS and remote sensing in NW Ethiopia. *Geoderma Regional*, 12, 83-
847 90, 2018.
- 848 Zhang, D. S.: The calculation of urban soil erosion based on GIS-a case study of Wuhan City.
849 Southwest University of M.S.Dissertation, 2011 (in Chinese).
- 850 Zhang, H., Liao, X. L., Zhai, T. L.: Evaluation of ecosystem service based on scenario simulation
851 of land use in Yunnan Province. *Physics and Chemistry of the Earth, Parts A/B/C*. 2017.
- 852 Zhang, T., Jin, D. G., Dong, G. C., Lin, J., Tang, P., Li, L. P.: Monitoring Soil Erosion in Linear
853 Production and Construction Project Areas Based on RUSLE-A Case Study of North Ring
854 Expressway in Ningbo City, Zhejiang Province. *Bulletin of Soil and Water Conservation*,
855 36(5): 131-135, 2016 (in Chinese).
- 856 Zhang, T., Jin, D. G., Tong, G. C., Lin, J., Tang, P., Li, L. P.: Monitoring Soil Erosion in Linear
857 Production and Construction Project Areas Based on RUSLE - A Case Study of North Ring
858 Expressway in Ningbo City, Zhejiang Province. *Bulletin of Soil and Water Conservation*,
859 36(5):131-135, 2016 (in Chinese).
- 860 Zhao, C. C., Ding, Y. J., Ye, B. S., Zhao, Q. D.: Spatial distribution of precipitation in Tianshan
861 Mountains and its estimation. *Advance in water science*, 22:315-322, 2011 (in Chinese)
- 862 Zhao, L., Yuan, G. L., Zhang, Y., He, B., Liu, Z. H., Wang, Z. Y., Li, J.: The Amount of Soil
863 Erosion in Baoxiang Watershed of Dianchi Lake Based on GIS and USLE. *Bulletin of Soil*

- 864 and Water Conservation, 27(3): 42-46, 2007 (in Chinese).
- 865 Zhou, F. C.: Highway Slope Ecological Protection Against Erosion Mechanism and Control Effect
866 Research. Chongqing jiaotong university, 2010 (in Chinese).
- 867 Zhou, R. G., Zhong, L. D., Zhao, N. L., Fang, J., Chai, H., Jian, Z., Wei, L., Li. B.: The
868 Development and Practice of China Highway Capacity Research. Transportation Research
869 Procedia, 15: 14-25, 2016.
- 870 Zhou, R. G., Zhong, L. D., Zhao, N. L., Fang, J., Chai, H., Jian, Z., Wei, L., Li. B.: The
871 Development and Practice of China Highway Capacity Research. Transportation Research
872 Procedia, 15: 14-25, 2016.
- 873 Zhu, J., Li, Y. M., Jiang, D. M.: A Study on Soil Erosion in Alpine and Gorge Region Based on
874 GIS and RUSLE Model-Taking Lushui County of Yunnan Province as an Example. Bulletin
875 of Soil and Water Conservation, 36(3): 277-283, 2016 (in Chinese).
- 876 Zhu, S. Q., Lin, J. L., and Lin, W. L.: Preliminary Study on Effects of Expressway Construction on
877 Side-Slope Soil Erosion in Mountainous Areas. Resources Science, 26(1):54-60, 2004 (in
878 Chinese).
- 879 Zhuo, M. N., Li, D. Q., and Zheng, Y. J.: Study on Soil and Water Conservation Effect of
880 Bioengineering Techniques for Slope Protection in Highway. Journal of Soil and Water
881 Conservation, 20(1):164-167, 2006 (in Chinese).